iScience

CellPress

Article

Overcome Competitive Exclusion in Ecosystems

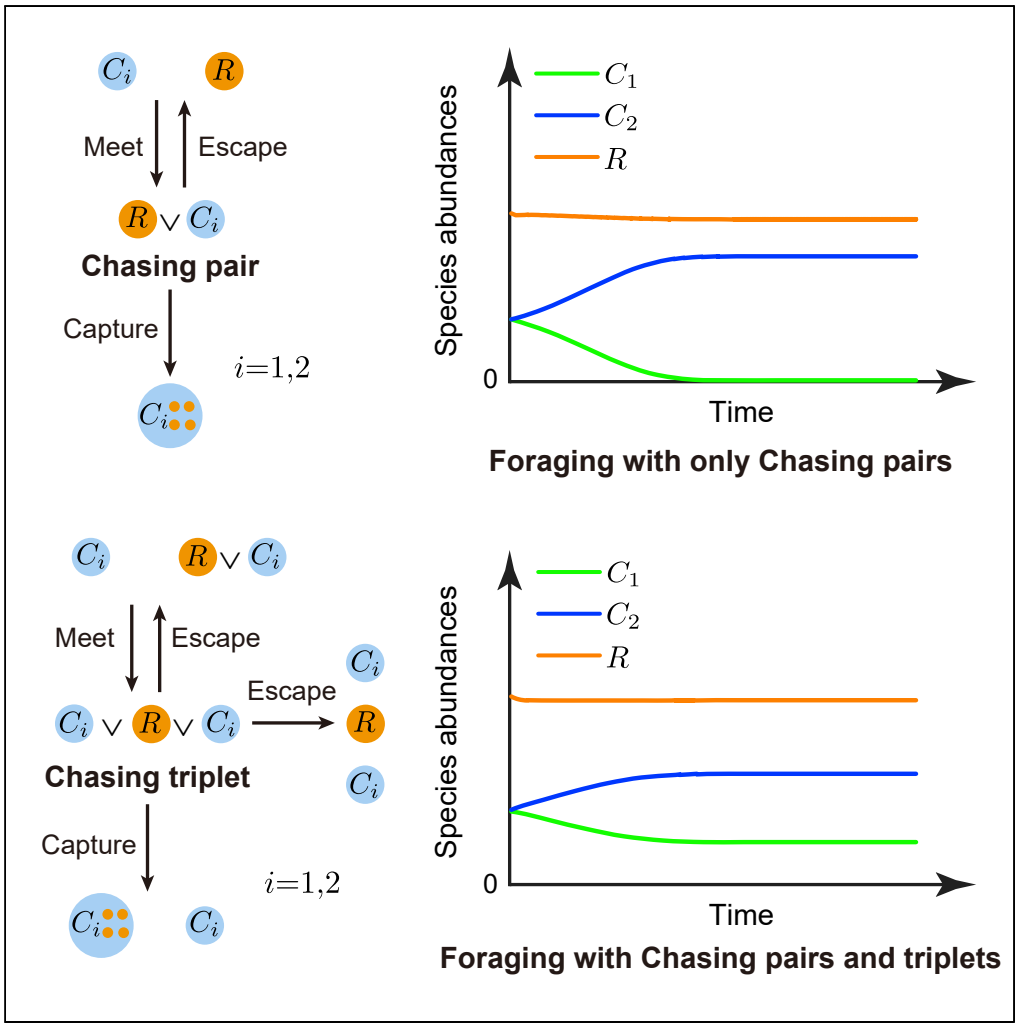

Xin Wang, Yang-Yu Liu

yyl@channing.harvard.edu

HIGHLIGHTS

Foraging with only chasing pairs cannot break the Competitive Exclusion Principle (CEP)

A population dynamics model involving both chasing pairs and triplets can break CEP

Redundant foraging within the chasing triplets facilitates species coexistence

The theoretical framework is testable in ecosystems involving pack hunting

Wang & Liu, iScience *23*, 101009
April 24, 2020
https://doi.org/10.1016/j.isci.2020.101009

iScience

CellPress

Article

Overcome Competitive Exclusion in Ecosystems

Xin Wang[1,2] and Yang-Yu Liu[1,3,4,*]

SUMMARY

Explaining biodiversity in nature is a fundamental problem in ecology. An outstanding challenge is embodied in the so-called Competitive Exclusion Principle: two species competing for one limiting resource cannot coexist at constant population densities, or more generally, the number of consumer species in steady coexistence cannot exceed that of resources. The fact that competitive exclusion is rarely observed in natural ecosystems has not been fully understood. Here we show that, by forming chasing pairs and chasing triplets among the consumers and resources in the consumption process, the Competitive Exclusion Principle can be naturally violated. The modeling framework developed here is broadly applicable and can be used to explain the biodiversity of many consumer-resource ecosystems and hence deepens our understanding of biodiversity in nature.

INTRODUCTION

In Darwin's theory of evolution, survival of the fittest, i.e., the less competitive species die out, implicating the notion of competition exclusion (Darwin, 1859). In 1928, Volterra illustrated mathematically that when two species compete for a single resource, one must die out unless the hunting to death rate ratio is exactly the same for the two competing species (Volterra, 1928). Those results were absorbed in the famous Competition Exclusion Principle (CEP) (Hardin, 1960; Gause, 1934; Armstrong and McGehee, 1980), also named as Gause's law (Gause, 1934): two species competing for one type of resource cannot coexist at steady state. In the 1960s, MacArthur and Levins extended this principle to ecosystems with arbitrary number of resource species (MacArthur and Levins, 1964; Levin, 1970; McGehee and Armstrong, 1977). Consider M types of consumer species competing for N types of resources. Each consumer can feed on one or multiple types of resources. Consumers do not directly interact with each other via other mechanisms except competing for the resources. According to the CEP (MacArthur and Levins, 1964; Levin, 1970; McGehee and Armstrong, 1977), at steady state the number of coexisting species of consumers cannot exceed that of resources, i.e., $M \leq N$ (see also Figure S1).

The classical proof (MacArthur and Levins, 1964; Levin, 1970; McGehee and Armstrong, 1977) of the CEP is demonstrated in Figure 1. Consider the simplest case: $M = 2$ and $N = 1$, i.e., two consumer species C_1 and C_2 compete for one type of resource R (Figure 1A). The generic population dynamics of this consumer-resource system can be described as follows:

$$\begin{cases} \dot{C}_i = C_i(f_i(R) - D_i), \quad i = 1, 2; \\ \dot{R} = g(R, C_1, C_2). \end{cases} \qquad \text{(Equation 1)}$$

Here f_i and g are unspecified functions, D_i stands for mortality rate of the consumer C_i. At steady state, if the two consumer species coexist, we have $f_i(R) = D_i$, $i = 1, 2$. This requires that the two curves $y = f_1(R)/D_1$ and $y = f_2(R)/D_2$ should cross the line $y = 1$ at the same point, which is typically impossible (Figure 1B), unless the model parameters satisfy certain constraint (with Lebesgue measure zero, see Figure S2B). Hence, generically the two consumer species cannot coexist at steady state (Figure 1C). In the case of $M = 3$, $N = 2$, the general population dynamics of the system can be written as

$$\begin{cases} \dot{C}_i = C_i(f_i(R_1, R_2) - D_i), \quad i = 1, 2, 3; \\ \dot{R}_j = g_j(R_1, R_2, C_1, C_2, C_3), \quad j = 1, 2. \end{cases} \qquad \text{(Equation 2)}$$

Here f_i and g_j are unspecified functions. Similar proof strategy used in the case of $M = 2$ and $N = 1$ can be applied here (see Figures 1D–1F and S2A), or more complicated cases with any positive N and M (MacArthur and Levins, 1964).

Interestingly, an astonishing level of biodiversity has been witnessed in most natural ecosystems. In aquatic biology, Hutchinson first proposed the paradox of the plankton: a limited number of resource types supports an unexpectedly large number of plankton species (Hutchinson, 1961). In tropical rainforests, one gram of soil contains a spectacular 2,000 to 18,000 distinct microbial genomes (Daniel, 2005). The vast diversity of microbial

[1]Channing Division of Network Medicine, Brigham and Women's Hospital and Harvard Medical School, Boston, MA 02115, USA

[2]School of Physics, Sun Yat-Sen University, Guangzhou 510275, China

[3]Center for Cancer Systems Biology, Dana-Farber Cancer Institute, Boston, MA 02115, USA

[4]Lead Contact

*Correspondence: yyl@channing.harvard.edu

https://doi.org/10.1016/j.isci.2020.101009

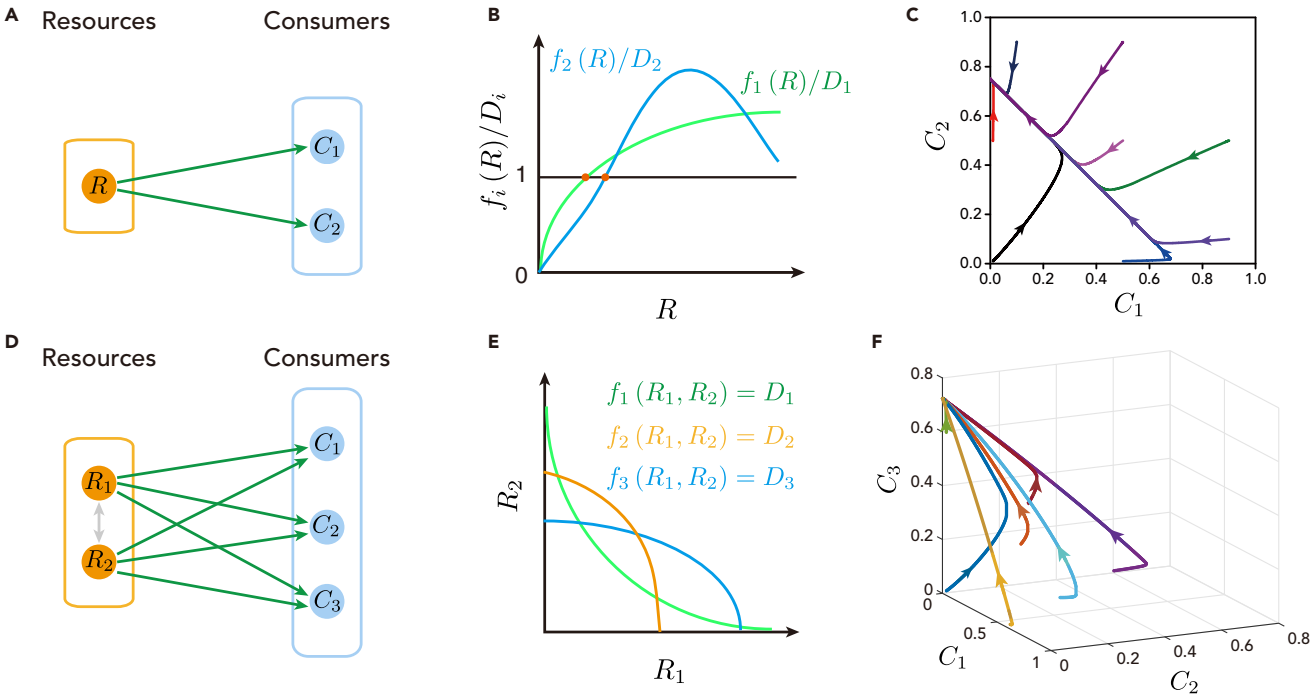

Figure 1. Classical proof of the Competitive Exclusion Principle

(A) The scenario of two consumer species ($M = 2$) and one resource species ($N = 1$). The green arrows denote the biomass flow among the consumption relationships.

(B) At steady state, if the two consumer species coexist, then according to Equation 1, $f_i(R)/D_i = 1$ ($i = 1, 2$). This requires that the following three lines $y = f_i(R)/D_i (i = 1, 2)$ and $y = 1$ intersect at a single point, which normally cannot happen.

(C) Representative trajectories of the two consumer species, which cannot coexist at steady state when $N = 1$. Here $f_i(R) = \alpha R$ ($i = 1, 2$); $g(R, C_1, C_2) = R(r^{(0)} - \beta^{(0)} R - \beta^{(1)} C_1 - \beta^{(2)} C_2)$ See Table S1 for simulation details.

(D) The scenario of three consumer species ($M = 3$) and two resource species ($N = 2$). Predation or other interactions are forbidden among consumers but allowed (denoted by gray arrows) among resources.

(E) If the three consumer species coexist at steady state, then according to Equation 2, $f_i(R_1, R_2) = D_i$ ($i = 1, 2, 3$). Generically, three curves would not intersect at exactly the same point, hence the three consumer species cannot coexist at steady state.

(F) Representative trajectories of the three consumer species, which cannot all coexist at steady state (see Figure S2A for the case that two of the three consumer species coexist). Here $f_i(R_1, R_2) = \alpha_i^{(1)} R_1 + \alpha_i^{(2)} R_2$ ($i = 1, 2, 3$); $g_j(R_1, R_2, C_1, C_2, C_3) = R_j(r_j^{(0)} - \beta_j^{(0)} R_j - \beta_j^{(1)} C_1 - \beta_j^{(2)} C_2 - \beta_j^{(3)} C_3)$ ($j = 1, 2$). See Table S1 for simulation details. See also Figures S1 and S2.

species plays an important role in the biogeochemical nutrient cycling of our planet. Yet, how could this biodiversity naturally emerge and sustain? Explaining biodiversity is a great challenge in ecology. In the past five decades, many mechanisms have been proposed to overcome the limitation on biodiversity set by CEP. Some argued that ecosystem never approaches steady state due to temporal (Hutchinson, 1961; Levins, 1979; Descamps-Julien and Gonzalez, 2005) or spatial factors (Levin, 1974; Richerson et al., 1970) or species self-organized dynamics (Koch, 1974; Huisman and Weissing, 1999; Benincà et al., 2008). Some considered special cases when the system parameters satisfy certain constraints (Volterra, 1928). The rest considered aspects such as cross-feeding (Turner et al., 1996; Goyal and Maslov, 2018; Goldford et al., 2018), toxin (Czárán et al., 2002), rock-paper-scissors relation (Kerr et al., 2002; Kelsic et al., 2015; Grilli et al., 2017), predator interference (Skalski and Gilliam, 2001; Beddington, 1975; Crowley and Martin, 1989; DeAngelis et al., 1975; Kuang et al., 2003), complex interactions (Kelsic et al., 2015; Bairey et al., 2016; Grilli et al., 2017), metabolic trade-off (Posfai et al., 2017), or co-evolution (Xue and Goldenfeld, 2017) (see Supplemental Information Sec.II.A for details).

Many of the mechanisms mentioned above are broadly relevant to promote biodiversity in nature. In the context of CEP itself, here we present a mechanism that considers the details of the consumption process. Specifically, consumer and resource species can form a chasing pair when an individual consumer is chasing an individual resource, whereas they form a chasing triplet when two individuals of consumer chase an individual resource simultaneously. We find that forming chasing pairs and chasing triplets among the consumers and resources can naturally break the CEP and hence facilitate biodiversity.

RESULTS

Consumption Process with Chasing Pairs

We realize that none of the previous studies explicitly considered the detailed consumption process. Although the timescale of the consumption process is generally much faster than that of the birth and death processes, it can have remarkable impact on the population dynamics (see Supplemental Information Sec.III.B for details). Hence, in our modeling framework, we explicitly consider the consumption process between the consumers and resources (see Figure S3A). The consumers are biotic (i.e., living organisms), whereas the resources can be either biotic or abiotic (i.e., supplied nutrients that are not alive). First, we consider the case that both consumer species and resource species are biotic, and for simplicity we assume both species are motile. Then we can explicitly consider the population structure of consumers and resources: some are wandering around freely; some are chasing each other. When a consumer encounters a resource with rate a, they form a chasing pair, denoted as $R^{(P)} \vee C^{(P)}$, where the superscript "P" stands for "pair." The resource can either "escape" with rate d or be caught and consumed by the consumer with rate k. For abiotic resources, they cannot actively escape from the consumers, yet they may passively "escape" owing to environmental factors. In this case, the "escape" rate corresponds to that the consumer fails to capture the resource in a chasing pair, which is analogous to a non-effective collision in chemical reactions. Such a consumption kinetics commonly takes the Michaelis-Menten form:

$kC\frac{R}{R+K}$, with $K \equiv \frac{d+k}{a}$, which corresponds to the Holling's type-II functional response (Holling, 1959) in ecology and is widely adopted in consumer-resource models (Koch, 1974; Momeni et al., 2017). This form, in fact, agrees with the growth rate function in the classical proof (MacArthur and Levins, 1964; Levin, 1970; McGehee and Armstrong, 1977), where $f(R) = wk\frac{R}{R+K}$ and w is a biomass conversion ratio constant (see Supplemental Information Sec.III.B for details). Nevertheless, the Michaelis-Menten kinetics is a good approximation only if the resource population is much larger than the consumer population, i.e., $R \gg C$.When this condition is not satisfied, the growth rate function follows $f(R, C)$ (Liu et al., 2015) rather than $f(R)$ (see Supplemental Information Sec.III.A for details). The C-dependency in the growth rate function invalidates the classical proof (MacArthur and Levins, 1964; Levin, 1970; McGehee and Armstrong, 1977), implying a potential mechanism to break the CEP. Actually, existing mechanisms involving predator interference (Skalski and Gilliam, 2001; Beddington, 1975; Crowley and Martin, 1989; DeAngelis et al., 1975) or ratio-dependent predation (Arditi and Ginzburg, 1989; Abrams and Ginzburg, 2000) also have C-dependency in the growth rate function or functional response.

Forming Chasing Pairs Still Cannot Break the CEP

Interestingly, we find that the presence of chasing pair and the C-dependent growth rate functions are still not enough to break the CEP. For example, in case $M = 2$ and $N = 1$ (Figure 2A), the population dynamics of the system can be described as follows:

$$\begin{cases} \dot{x}_i = a_i R^{(F)} C_i^{(F)} - (d_i + k_i)x_i, \\ \dot{C}_i = w_i k_i x_i - D_i C_i, \\ \dot{R} = g(R, x_1, x_2, C_1, C_2), \end{cases} \quad \text{(Equation 3)}$$

with $i = 1, 2$. Here consumers and resources that are freely wandering around are denoted as $C_i^{(F)}$ and $R^{(F)}$, respectively, where the superscript "F" stands for "freely wandering." The variable $x_i \equiv R^{(P)} \vee C_i^{(P)}$ represents the chasing pair, a_i is the encounter rate between a consumer C_i and a resource to form a chasing pair x_i, d_i is the "escape" rate of a resource out of a chasing pair x_i, and k_i is the capture rate of consumer C_i in a chasing pair x_i. If the two consumers can coexist, we prove that the steady-state equations yield $f_i(R^{(F)})/D_i = 1$, with $f_i(R^{(F)}) \equiv \frac{R^{(F)}}{R^{(F)} + K_i}$ and $K_i \equiv \frac{d_i + k_i}{a_i}$ (see Supplemental Information Sec.IV for details), which corresponds to parallel planes in the $(C_1, C_2, R^{(F)})$ coordinate system (Figure S3C), rendering coexistence impossible (Figures 2C, 2E, and S3, see Supplemental Information Sec.IV-V for details).

Consumption Process with Chasing Triplets

Pack hunting is prevalent across different organisms in the wild (Creel and Creel, 1995; Muro et al., 2011; Geisen et al., 2015; Merron, 1993; Stander, 1992; Boesch, 1994; Bshary et al., 2006; Vail et al., 2013; Berleman and Kirby, 2009; Seccareccia et al., 2015). Intraspecific pack hunting is very general and commonly occurs, whereas interspecific pack hunting has also been reported for a handful of species (Bshary et al., 2006; Vail et al., 2013). This means that two or more consumer individuals can chase the

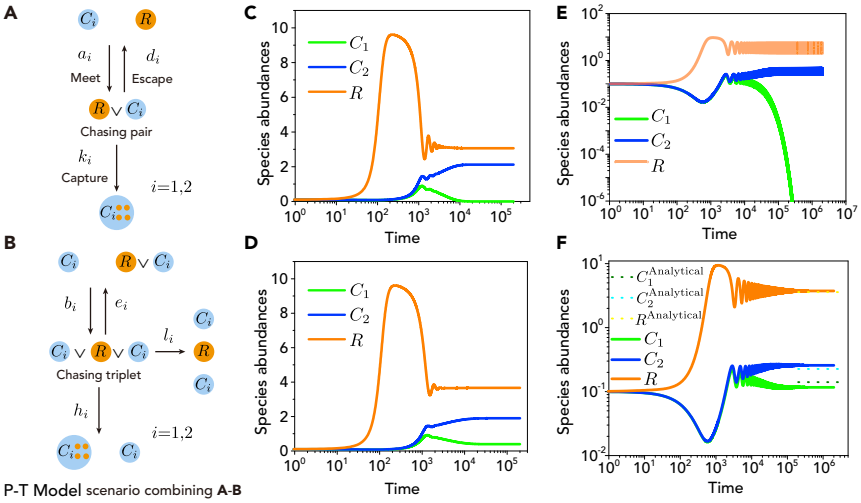

Figure 2. Modeling the Consumption Process between Consumers and Resources Explicitly May Naturally Break the CEP

For simplicity, we consider the case of two consumer species ($M = 2$) and one biotic resource species ($N = 1$, see Figures S5C and S5D for the case of abiotic resource species).

(A) Formation of a chasing pair between a consumer and a resource.

(B) Formation of a chasing triplet among two consumers of the same species and a resource. We denote the scenario combining chasing pair (A) and triplet (B) as P-T Model.

(C and E) Time courses of the species abundances involving only chasing pair. (C) Consumer species cannot coexist at steady state. (E) Only one type of consumer species exists for long, the oscillating dynamics resembles that of the classical predator-prey models (May, 1972).

(D and F) Time courses of the species abundances in P-T Model with the presence of chasing pairs and chasing triplet. Both consumer species can coexist at steady state. The dotted lines in (F) are the steady-state analytical solutions (labeled with superscript "Analytical") calculated in Equations S30–S32. (C) and (E) were simulated from Equation 3, where $g = RR_0(1 - R/K_0) - (k_1x_1 + k_2x_2)$. (D) and (F) were simulated from Equations 4 and 5.

See Table S1 for simulation details. See also Figures S3–S10.

same resource individual simultaneously. To take this into account, we revisit the consumption process and naturally extend the idea of chasing pair to chasing triplet, i.e., two consumers (within the same or from different species) can chase the same resource (Figures 2B and S4). For intraspecific pack hunting, in case $M = 2$ and $N = 1$, a consumer C_i can join an existing chasing pair $x_i \equiv R^{(P)} \vee C_i^{(P)}$ to form a chasing triplet $y_i \equiv C_i^{(T)} \vee R^{(T)} \vee C_i^{(T)}$ (Figure 2B, in combination with Figure 2A, denoted as P-T Model), where the superscript "T" stands for "triplet." The population of consumers and resources consists of freely wandering individuals ($C_i^{(F)}$, $R^{(F)}$) and those involved in a chasing pair (x_i) or triplet (y_i). Mathematically, they are given by $C_i = C_i^{(F)} + x_i + 2y_i$ ($i = 1, 2$) and $R = R^{(F)} + \sum_{i=1}^{2}(x_i + y_i)$, respectively. The population dynamics of the system can be described as follows:

$$\begin{cases} \cdot\ x_i = a_i R^{(F)} C_i^{(F)} - (d_i + k_i)x_i - b_i x_i C_i^{(F)} + e_i y_i, \\ \cdot\ y_i = b_i x_i C_i^{(F)} - (h_i + e_i + l_i)y_i, \\ \cdot\ C_i = w_i(k_i x_i + h_i y_i) - D_i C_i, \\ \dot{R} = g(R, x_1, x_2, y_1, y_2, C_1, C_2), \end{cases} \qquad \text{(Equation 4)}$$

with $i = 1, 2$. Here b_i is the encounter rate between a consumer C_i and an existing chasing pair x_i to form a chasing triplet y_i; e_i and l_i are the escape rates of a consumer C_i out of a chasing triplet y_i (Figure 2B). Consumer species C_i can capture resource R either from a chasing pair x_i with rate k_i or from a triplet y_i with rate h_i.

Forming Both Chasing Pairs and Chasing Triplets Can Break the CEP

In Equation 4, the explicit form of function $g(R, x_1, x_2, y_1, y_2, C_1, C_2)$ is not specified. We assume that the dynamics of the resources follow the same construction principle as that in the classical MacArthur's consumer-resource model (MacArthur, 1970; Chesson, 1990). Then,

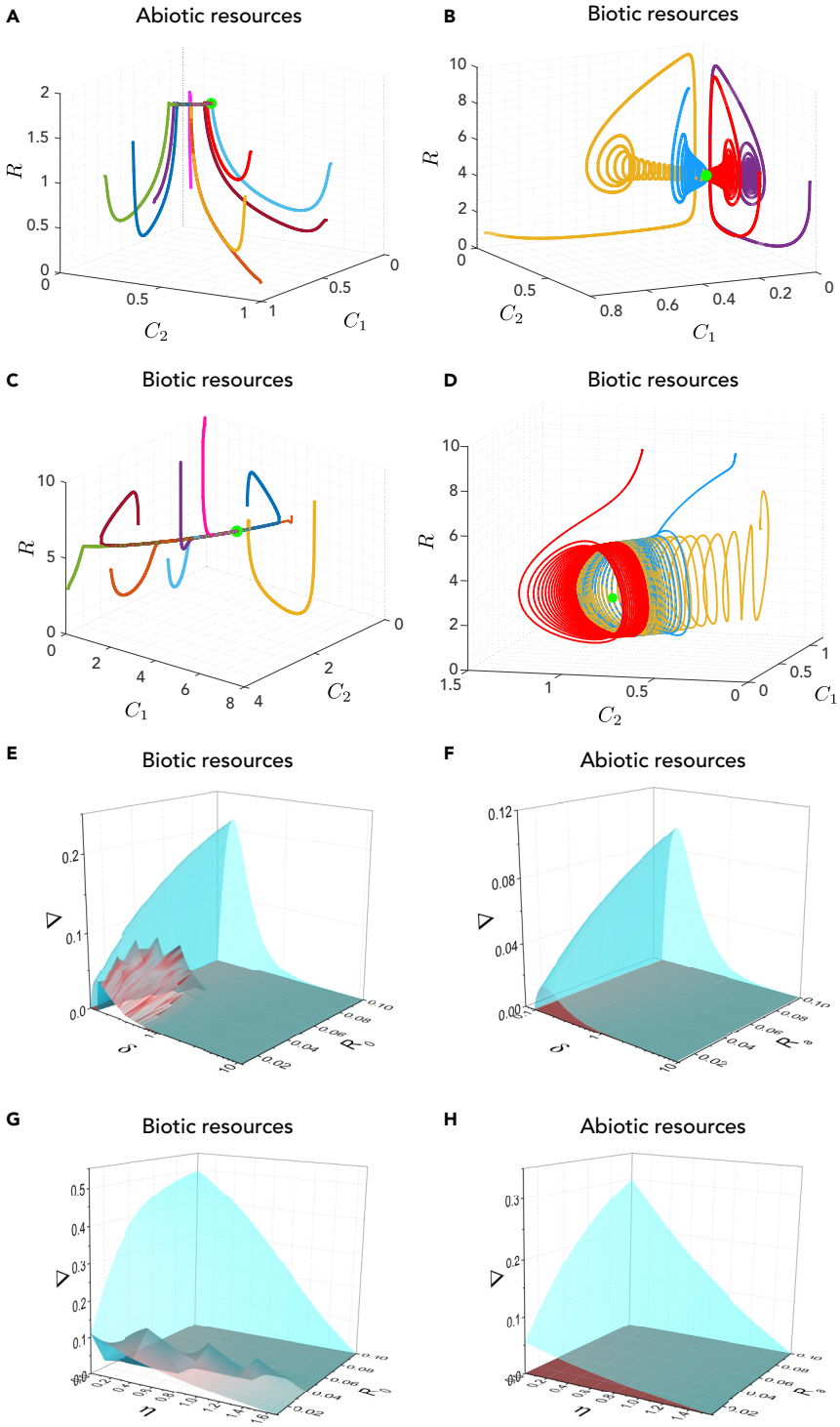

Figure 3. Coexistence of Two Consumer Species ($M = 2$) and One Resource Species ($N = 1$) within the P-T Model

(A–D) Different types of coexistence trajectories in the state space. (A) Abiotic resource case, the coexistence state (green dot) is globally attracting. (B–D) Biotic resource cases, green dot marks the fixed point. (B), (C) The coexistence state is globally attracting. (D) The coexistence state is unstable; all trajectories attract to a stable limit cycle.

(E–H) Stable coexistence region in the P-T Model. D_i ($i = 1, 2$) is the only different parameter between consumer species C_1 and C_2, and $\Delta \equiv (D_1 - D_2)/D_2$, the relative difference in mortality rate, measures the competitive differences between the two consumer species. δ in (E) and (F) is a dimensionless multiplier that to tune the capture rate and escape rate

Figure 3. *Continued*

parameters for the two-consumer species in each scenario. η in (G) and (H) is a dimensionless multiplier that to tune h_i (i = 1,2), the capture rate in the chasing triplet for the two consumer species. The regions below the blue surface and above the red surface are stable coexistence region, whereas the regions below the red surface and above $\Delta = 0$ are the regions for unstable fixed point, where trajectories typically end in a limit cycle (see also Figure S8 and Supplemental Information Sec.V.D). (E) and (G) Biotic resource cases. (F) and (H) Abiotic resource cases. (A)–(D) were simulated from Equations 4 and 5. (E)–(H) were calculated from Equations 4 and 5.
See Table S1 for simulation and calculation details. See also Figure S8.

$$g(R, x_1, x_2, y_1, y_2, C_1, C_2) = \begin{cases} RR_0(1 - R/K_0) - (k_1x_1 + k_2x_2) - (h_1y_1 + h_2y_2), \\ \qquad\qquad\qquad\qquad\qquad\qquad \text{for biotic resources.} \\ R_a(1 - R/K_0) - (k_1x_1 + k_2x_2) - (h_1y_1 + h_2y_2), \\ \qquad\qquad\qquad\qquad\qquad\qquad \text{for abiotic resources.} \end{cases} \quad \text{(Equation 5)}$$

Biotic resources take logistic population growth in the absence of consumers, hence R_0 represents the intrinsic growth rate (with dimension 1/time) and K_0 represents the carrying capacity. Abiotic resources are supplied externally, then R_a stands for the external resource supply rate (with dimension mass/time) and K_0 is the steady state resource abundance in the absence of consumers.

Using dimensional analysis, we make all parameters dimensionless (see Supplemental Information Sec.VII for details). For convenience, below we still use the same parameter notations, yet they are all dimensionless. Actually, K_0 and D_2 are two reducible parameters (see Supplemental Information Sec.VII for details); for convenience, we set $K_0 = 10$ and $D_2 = 0.005$ for biotic resource cases, whereas $K_0 = 5$ and $D_2 = 0.004$ for abiotic resource cases. In the numerical simulations of the P-T Model (Figures 2A and 2B), we find that two consumer species can achieve steady coexistence when there is only one type of resource (Figures 2D, 2F, and S5D), which naturally breaks the CEP.

When the abundance of resources are much larger than that of consumers (i.e., $R \gg C_1, C_2$), which generally hold in most natural ecosystems, the steady-state population of the consumer species and resource species can be analytically calculated (see Supplemental Information Sec.V.B for details). In Figures 2F and S6, we show that the steady-state analytical results of both biotic and abiotic resource cases agree well with numerical results.

Interestingly, there are several types of coexistence trajectories in phase space within the scenario of P-T Model, which involves chasing pair and triplet formed between consumers of the same species. When the resource is abiotic, there is only one type of behavior: the coexistence state is globally attracting as long as the initial abundances of these species are non-zero, as shown in Figure 3A. However, in the case that the resource is biotic, the coexistence state can be either globally attracting (Figures 3B and 3C) or unstable, leading to a limit cycle (Figure 3D) (see Figure S5B for the oscillating coexistence in time series). In some cases, the oscillations damps, and ends in the globally attracting fixed point, as shown in Figure 3B.

We further considered scenarios involving interspecific group (Bshary et al., 2006; Vail et al., 2013), specifically, two variants of the P-T Model, where the chasing triplet is formed between different species of consumers (Figure S4A) or either between the same or different species (Figure S4B). In both Variants, two consumer species can coexist either steadily (Figures S7A and S7C) or with sustained oscillations (Figures S7B and S7D) when there is only one type of resource species (see Supplemental Information Sec.V.C for details).

To verify that our findings are not due to accidental model parameters, we systematically studied the parameter space for stably steady coexistence. We found that, for both the P-T Model and its two variants, regardless of biotic or abiotic resources, there exists a non-zero parameter space where the two consumer species can stably steadily coexist with one type of resource species (see Figures 3E–3H and S8 and Supplemental Information Sec.V.D for details), demonstrating that the violation of CEP is not due to a special set of model parameters. Note that the violation of CEP in the case of $N = 1$ actually implies that it will be violated for more general cases with $N > 1$ (see Supplemental Information Sec.VI for details).

Intuitive Explanation of Why Forming Chasing Pairs and Chasing Triplets Can Break the CEP

A simple explanation is that a resource within a chasing pair can be effectively regarded as another species when forming a chasing triplet (e.g., R within $R^{(P)} \vee C^{(P)}$ in Figure 2B), although in essence, they still remain

the same identity. In the P-T Model, consumer species C_i can get resource R in two ways, potentially with different effective capture rates in a chasing pair or a chasing triplet. As a rough estimate, the resource abundance in a chasing pair ($R^{(P)} \vee C_i^{(P)}$) is proportional to RC_i, whereas in a chasing triplet ($C_i^{(T)} \vee R^{(T)} \vee C_i^{(T)}$) it is proportional to RC_i^2. Here R and C_i are the total populations of resource R and consumer C_i, respectively. Thus, when C_i becomes higher, it obtains a higher fraction of resource from a chasing triplet. If the effective capture rate in a chasing triplet is lower than that in a chasing pair, implying a wasteful or redundant foraging, then this gives rise to an auto-suppression on the intraspecific growth rate, which can facilitate species coexistence (Chesson, 2000). Without loss of generality, let's assume that C_2 is more competitive than C_1, in obtaining the resource from either a chasing pair or triplet; however, C_1 can be more effective in obtaining the resource from chasing pair $R^{(P)} \vee C_1^{(P)}$ than C_2 from chasing triplet $C_2^{(T)} \vee R^{(T)} \vee C_2^{(T)}$ owing to redundant foraging. When the population of C_2 is larger than that of C_1, higher fraction of C_2 is involved in the less effective chasing triplet foraging, which may lead to an overall balanced competitiveness between the two consumer species at such population densities (with $C_2 > C_1$) and thus facilitates species coexistence. If this redundant foraging hypothesis is correct, then the less effective the chasing triplet foraging is, the easier it is for the two consumer species to coexist. In other words, the two consumer species can coexist with a larger competitiveness difference (see Supplemental Information section V.D and Figure S8C for details). To test this redundant foraging hypothesis, we set D_i to be the only different parameter between consumer species C_1 and C_2, and specifically tune h_i, the capture rate in a chasing triplet with a multiplier η: $h_i = \eta h_i^{(0)}$, where $h_i^{(0)} = k_i$ and k_i is the capture rate in a chasing pair. In Figures 3G and 3H, our systematical numerical results show that decreasing the capture rate in a chasing triplet indeed promotes species coexistence, where $\Delta \equiv (D_1 - D_2)/D_2$measures the competitiveness difference between the two consumer species. The supremum of Δ peaks at $\eta = 0$ and it decreases with increasing η for both biotic and abiotic resource cases (Figures 3G and 3H). These results fully support the redundant foraging hypothesis.

To offer a more quantitative explanation, we consider the functional forms of population dynamics at steady state. In the classical proof of CEP, in the case of $M = 2$ and $N = 1$ (Figures 1A–1C), if both consumers species can coexist at steady state, the abundance of the resource species R needs to satisfy two equations ($f_i(R)/D_i = 1$ ($i = 1, 2$)) simultaneously. This is equivalent to requiring that two parallel planes share a common point, which is typically impossible (Figure 4A). In the presence of chasing pairs, as shown in Figure 4B, the requirement for steady coexistence corresponds to parallel surfaces ($f_i(R^{(F)})/D_i = 1$ ($i = 1, 2$)), see Supplemental Information Sec.IV-V for details). In the presence of both chasing pairs and chasing triplets, as shown in Figure 4C, the requirement for steady coexistence corresponds to three non-parallel surfaces $\Omega_i(R, C_1, C_2) = D_i C_i (i = 1, 2)$, $g(R, C_1, C_2) = 0$ (see Supplemental Information Sec.V for details) to cross at one point, which can in principle happen and hence breaks the CEP. To verify the intuitive explanation, we resort to numerical solutions. Figures 4D, 4E, and S9 show the results, where the yellow, green, and blue surfaces are the exact solutions. The parallel green and blue surfaces in the cases of only chasing pairs are verified with Figure 4D, whereas the three non-parallel surfaces in scenarios involving both chasing pairs and chasing triplets are verified with Figures 4E and S9.

To provide deeper insights into the break of CEP, we argue that the competitive exclusion (i.e., $M \leq N$ at steady state) in the classical proof of CEP or the scenario involving only chasing pairs stems from the symmetry constraint of the equation form. In those scenarios, for $M = 2$ and $N = 1$, there exists a variable $U \equiv U(R, C_1, C_2)$ satisfying the symmetry constraint that $\Theta_i(U(R, C_1, C_2)) = D_i$ ($i = 1, 2$, where Θ_i is an unspecified function) for the steady-state population dynamics. In the classical proof $U = R$ (see Equation 1); in the scenario involving only chasing pairs, $U = R^{(F)}$ (see Equations 3 and S13). The existence of U directly leads to parallel planes/surfaces (see Figures 4A, 4B, 4D, and S3C) and thus precludes consumer species coexistence. However, scenario involving both chasing pairs and chasing triplets or even higher-order terms (e.g., quadruplets, quintuplets) breaks the symmetry constraint in the equation form so that the variable $U \equiv U(R, C_1, C_2)$ does not exist; otherwise, there cannot be any intersection points in Figure 4E or Figure S9 (see Supplemental Information Sec.V.A.2 for details). This symmetry breaking enables the break of the CEP.

DISCUSSION

Over the past several decades, various mechanisms have been proposed to overcome the constraint on biodiversity set by CEP. Mechanisms such as temporal or spatial factors, self-organized dynamics, cross-feeding, and predator interference are likely to play significant role in maintaining the biodiversity in nature. Here, within the original context of CEP, by considering the details of the consumption process,

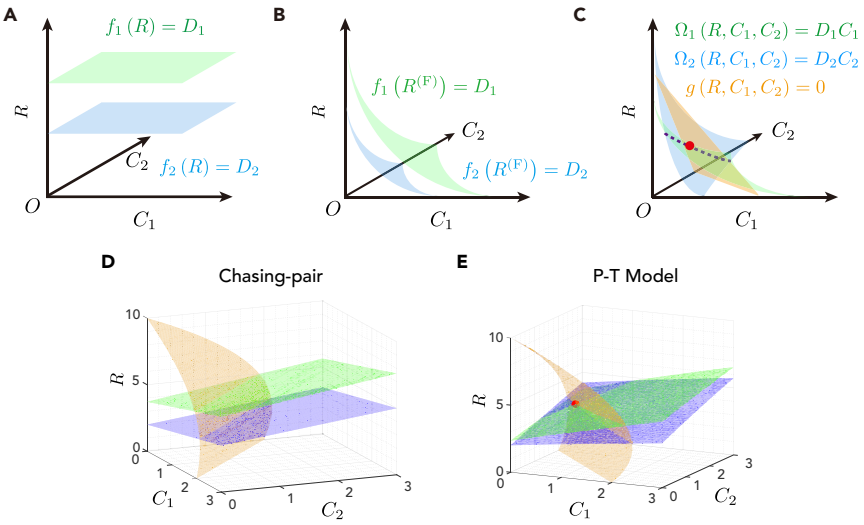

Figure 4. Intuitive Explanation of why the Formation of Chasing Triplet Can Break the CEP

For simplicity, we consider the case of $M = 2$ and $N = 1$.

(A) In the classical proof, the green plane and blue plane are parallel to each other and thus do not have a common point.

(B) In the model involving chasing pairs, the green surface and blue surface are still parallel to each other and thus still do not have a common point (see Figure S3C, Supplemental Information Sec.IV-V for details).

(C) In the model involving both chasing pairs and chasing triplets, the yellow, green, and blue surfaces are not parallel to each other and thus the green and the blue ones can have an intersection curve (shown in dashed purple), whereas the three surfaces can intersect at one point (shown in red) and thus facilitate coexistence.

(D and E) Demonstration of the intuitive explanation with numerical solutions. (D) In the scenario involving only chasing pair, numerical solutions confirm that the green surface and blue surface are parallel to each other. (E) In scenarios involving both chasing pair and triplet (P-T Model), numerical solutions confirm that the yellow, green, and blue surfaces are not parallel to each other and definitely can have a common point (marked with red dot, see Figure 2D for time series). (D) was calculated from Equation 3, where $g = RR_0(1 - R/K_0) - (k_1x_1 + k_2x_2)$; (E) was calculated from Equations 4 and 5. See Table S1 for simulation details. See also Figures S9 and S10.

especially the formation of chasing pairs and triplets inspired by the prevalent phenomenon of pack hunting, our mechanism naturally breaks the constraint of the CEP. Furthermore, we show that there are non-special parameter sets (of non-zero measure) that break the CEP in all scenarios involving different forms of chasing triplets. Meanwhile, we notice that breaking CEP is parameter dependent (see Figure S10 and Supplemental Information Sec.V.E): for certain parameters, there is no feasible fixed point for coexistence, or the fixed point can be unstable (for biotic resource cases), which may end in a limit cycle.

The coexistence predicted in our model is testable in experiments. Both macro- and microscopic ecosystems involving pack hunting are potential candidates. For microbial ecosystems, it has been reported that some microorganisms, such as *Myxococcus xanthus* (Berleman and Kirby, 2009), ameba (Geisen et al., 2015), and *Lysobacter* (Seccareccia et al., 2015), can feed on other microorganisms through pack hunting. But the caveat is that microbial communities are typically shaped by metabolic cross-feeding (Goldford et al., 2018), which is not considered in our model. Hence special attention needs to be paid to disentangle the impacts of cross-feeding and pack hunting in breaking the CEP of microbial communities.

Limitations of the Study

This study shows that, by forming chasing pairs and chasing triplets among the consumers and resources in the consumption process, the CEP can be naturally violated. However, several limitations should be paid attention. *First*, there are non-special parameter settings that can break the CEP in scenarios involving chasing triplets. Yet, this is not true for certain parameter settings, especially when there is large competitiveness difference between consumer species. *Second*, our model framework does not consider other factors that can also promote biodiversity in nature such as temporal or spatial factors and cross-feeding. Special attention needs to be paid to disentangle these confounding factors in future experimental validations.

METHODS

All methods can be found in the accompanying Transparent Methods supplemental file.

DATA AND CODE AVAILABILITY

The authors confirm that the data and code supporting the findings of this study are accessible from the corresponding author upon reasonable request.

SUPPLEMENTAL INFORMATION

Supplemental Information can be found online at https://doi.org/10.1016/j.isci.2020.101009.

ACKNOWLEDGMENTS

Research reported in this publication was supported by grants R01AI141529, R01HD093761, UH3OD023268, U19AI095219, and U01HL089856 from National Institutes of Health, United States. We thank Babak Momeni, Serguei Saavedra, Chao Tang, Terry Hwa, and Nannan Zhao for helpful discussions. We also thank two anonymous reviewers for very insightful comments, which significantly improved our paper.

AUTHOR CONTRIBUTIONS

X.W and Y.-Y.L conceived and designed the project, developed the model, and wrote the paper. X.W. carried out all the analytical and numerical calculations.

DECLARATION OF INTERESTS

The authors declare no competing interests.

Received: December 21, 2019
Revised: March 4, 2020
Accepted: March 18, 2020
Published: April 24, 2020

REFERENCES

Abrams, P.A., and Ginzburg, L.R. (2000). The nature of predation: prey dependent, ratio dependent or neither? Trends Ecol. Evol. *15*, 337–341.

Arditi, R., and Ginzburg, L.R. (1989). Coupling in predator-prey dynamics: ratio-dependence. J. Theor. Biol. *139*, 311–326.

Armstrong, R.A., and McGehee, R. (1980). Competitive exclusion. Am. Nat. *115*, 151–170.

Bairey, E., Kelsic, E.D., and Kishony, R. (2016). High-order species interactions shape ecosystem diversity. Nat. Commun. *7*, 1–7.

Beddington, J.R. (1975). Mutual interference between parasites or predators and its effect on searching efficiency. J. Anim. Ecol. 331–340.

Benincà, E., Huisman, J., Heerkloss, R., Jöhnk, K.D., Branco, P., van Nes, E.H., Scheffer, M., and Ellner, S.P. (2008). Chaos in a long-term experiment with a plankton community. Nature *451*, 822–825.

Berleman, J.E., and Kirby, J.R. (2009). Deciphering the hunting strategy of a bacterial wolfpack. FEMS Microbiol. Rev. *33*, 942–957.

Boesch, C. (1994). Cooperative hunting in wild chimpanzees. Anim. Behav. *48*, 653–667.

Bshary, R., Hohner, A., Ait-el-Djoudi, K., and Fricke, H. (2006). Interspecific communicative and coordinated hunting between groupers and giant moray eels in the Red Sea. PLoS Biol. *4*, e431.

Chesson, P. (1990). MacArthur's consumer-resource model. Theor. Popul. Biol. *37*, 26–38.

Chesson, P. (2000). Mechanisms of maintenance of species diversity. Annu. Rev. Ecol. Syst. *31*, 343–366.

Creel, S., and Creel, N.M. (1995). Communal hunting and pack size in African wild dogs, Lycaon pictus. Anim. Behav. *50*, 1325–1339.

Crowley, P.H., and Martin, E.K. (1989). Functional responses and interference within and between year classes of a dragonfly population. J. North Am. Benthol. Soc. *8*, 211–221.

Czárán, T.L., Hoekstra, R.F., and Pagie, L. (2002). Chemical warfare between microbes promotes biodiversity. Proc. Natl. Acad. Sci. U S A *99*, 786–790.

Daniel, R. (2005). The metagenomics of soil. Nat. Rev. Microbiol. *3*, 470–478.

Darwin, C. (1859). The Origin of Species by Means of Natural Selection (John Murray).

DeAngelis, D.L., Goldstein, R., and O'neill, R.V. (1975). A model for tropic interaction. Ecology *56*, 881–892.

Descamps-Julien, B., and Gonzalez, A. (2005). Stable coexistence in a fluctuating environment: an experimental demonstration. Ecology *86*, 2815–2824.

Gause, G. (1934). The Struggle for Existence (The Williams & Wilkins company).

Geisen, S., Rosengarten, J., Koller, R., Mulder, C., Urich, T., and Bonkowski, M. (2015). Pack hunting by a common soil amoeba on nematodes. Environ. Microbiol. *17*, 4538–4546.

Goldford, J.E., Lu, N., Bajić, D., Estrela, S., Tikhonov, M., Sanchez-Gorostiaga, A., Segrè, D., Mehta, P., and Sanchez, A. (2018). Emergent simplicity in microbial community assembly. Science *361*, 469–474.

Goyal, A., and Maslov, S. (2018). Diversity, stability, and reproducibility in stochastically assembled microbial ecosystems. Phys. Rev. Lett. *120*, 158102.

Grilli, J., Barabás, G., Michalska-Smith, M.J., and Allesina, S. (2017). Higher-order interactions stabilize dynamics in competitive network models. Nature *548*, 210–213.

Hardin, G. (1960). The competitive exclusion principle. Science *131*, 1292–1297.

Holling, C.S. (1959). The components of predation as revealed by a study of small-mammal predation of the European pine sawfly. Can. Entomol. *91*, 293–320.

Huisman, J., and Weissing, F.J. (1999). Biodiversity of plankton by species oscillations and chaos. Nature *402*, 407–410.

Hutchinson, G.E. (1961). The paradox of the plankton. Am. Nat. *95*, 137–145.

Kelsic, E.D., Zhao, J., Vetsigian, K., and Kishony, R. (2015). Counteraction of antibiotic production and degradation stabilizes microbial communities. Nature *521*, 516–519.

Kerr, B., Riley, M.A., Feldman, M.W., and Bohannan, B.J. (2002). Local dispersal promotes biodiversity in a real-life game of rock–paper–scissors. Nature *418*, 171–174.

Koch, A.L. (1974). Competitive coexistence of two predators utilizing the same prey under constant environmental conditions. J. Theor. Biol. *44*, 387–395.

Kuang, Y., Fagan, W.F., and Loladze, I. (2003). Biodiversity, habitat area, resource growth rate and interference competition. Bull. Math. Biol. *65*, 497–518.

Levin, S.A. (1970). Community equilibria and stability, and an extension of the competitive exclusion principle. Am. Nat. *104*, 413–423.

Levin, S.A. (1974). Dispersion and population interactions. Am. Nat. *108*, 207–228.

Levins, R. (1979). Coexistence in a variable environment. Am. Nat. *114*, 765–783.

Liu, X., Wang, X., Yang, X., Liu, S., Jiang, L., Qu, Y., Hu, L., Ouyang, Q., and Tang, C. (2015). Reliable cell cycle commitment in budding yeast is ensured by signal integration. Elife *4*, e03977.

MacArthur, R. (1970). Species packing and competitive equilibrium for many species. Theor. Popul. Biol. *1*, 1–11.

MacArthur, R., and Levins, R. (1964). Competition, habitat selection, and character displacement in a patchy environment. Proc. Natl. Acad. Sci. U S A *51*, 1207.

May, R.M. (1972). Limit cycles in predator-prey communities. Science *177*, 900–902.

McGehee, R., and Armstrong, R.A. (1977). Some mathematical problems concerning the ecological principle of competitive exclusion. J. Differ. Equ. *23*, 30–52.

Merron, G. (1993). Pack-hunting in two species of catfish, Clavias gariepinus and C. ngamensis, in the Okavango Delta, Botswana. J. Fish Biol. *43*, 575–584.

Momeni, B., Xie, L., and Shou, W. (2017). Lotka-Volterra pairwise modeling fails to capture diverse pairwise microbial interactions. Elife *6*, e25051.

Muro, C., Escobedo, R., Spector, L., and Coppinger, R. (2011). Wolf-pack (*Canis lupus*) hunting strategies emerge from simple rules in computational simulations. Behav. Processes *88*, 192–197.

Posfai, A., Taillefumier, T., and Wingreen, N.S. (2017). Metabolic trade-offs promote diversity in a model ecosystem. Phys. Rev. Lett. *118*, 028103.

Richerson, P., Armstrong, R., and Goldman, C.R. (1970). Contemporaneous disequilibrium, a new hypothesis to explain the "Paradox of the Plankton". Proc. Natl. Acad. Sci. U S A *67*, 1710–1714.

Seccareccia, I., Kost, C., and Nett, M. (2015). Quantitative analysis of Lysobacter predation. Appl. Environ. Microbiol. *81*, 7098–7105.

Skalski, G.T., and Gilliam, J.F. (2001). Functional responses with predator interference: viable alternatives to the Holling type II model. Ecology *82*, 3083–3092.

Stander, P.E. (1992). Cooperative hunting in lions: the role of the individual. Behav. Ecol. Sociobiol. *29*, 445–454.

Turner, P.E., Souza, V., and Lenski, R.E. (1996). Tests of ecological mechanisms promoting the stable coexistence of two bacterial genotypes. Ecology *77*, 2119–2129.

Vail, A.L., Manica, A., and Bshary, R. (2013). Referential gestures in fish collaborative hunting. Nat. Commun. *4*, 1–7.

Volterra, V. (1928). Variations and fluctuations of the number of individuals in animal species living together. ICES J. Mar. Sci. *3*, 3–51.

Xue, C., and Goldenfeld, N. (2017). Coevolution maintains diversity in the stochastic "Kill the Winner" model. Phys. Rev. Lett. *119*, 268101.

iScience, Volume *23*

Supplemental Information

Overcome Competitive Exclusion in Ecosystems

Xin Wang and Yang-Yu Liu

Supplemental Figures

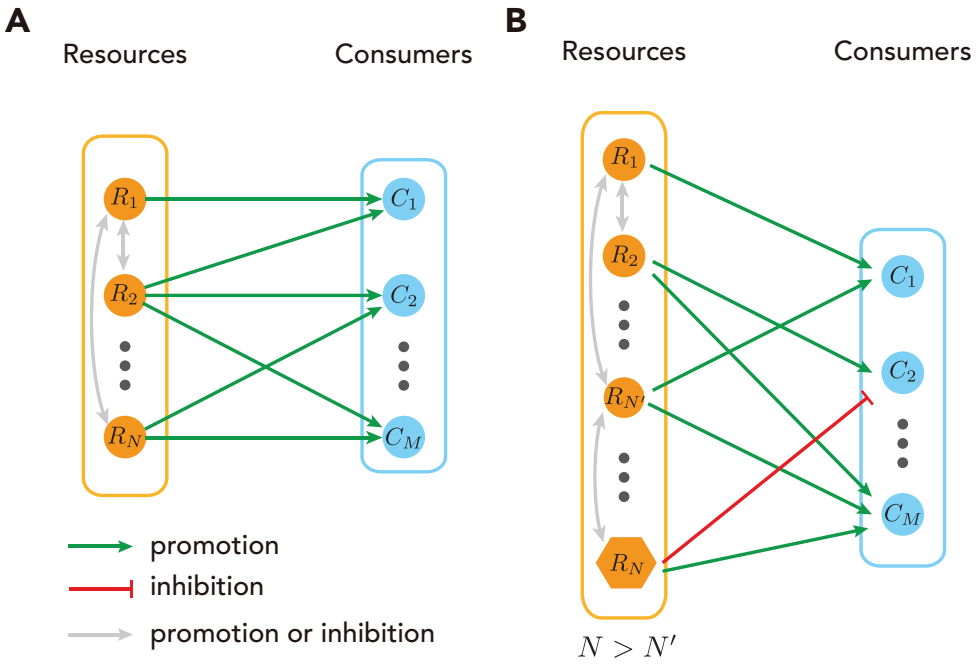

Figure S1: Bipartite graph between resources and consumers (Related to Figure 1).
(A) M species of consumers feed on N species of resources. Predation or other interactions are forbidden among consumers but allowed among resources. Competitive exclusion principle (CEP) states that at steady state the coexisting $M \leq N$. **(B)** Resources involve chemical compounds: R_i ($N' + 1 \leq i \leq N$; $N > N'$) are chemical compounds, which can promote or inhibit the growth of consumers, while R_i ($1 \leq i \leq N'$) are normal resources, supplying as food for consumers. In total, there are N species of resources and M species of consumers. According to CEP, at steady state, it is permitted that the coexisting $M > N'$, yet $M \leq N$.

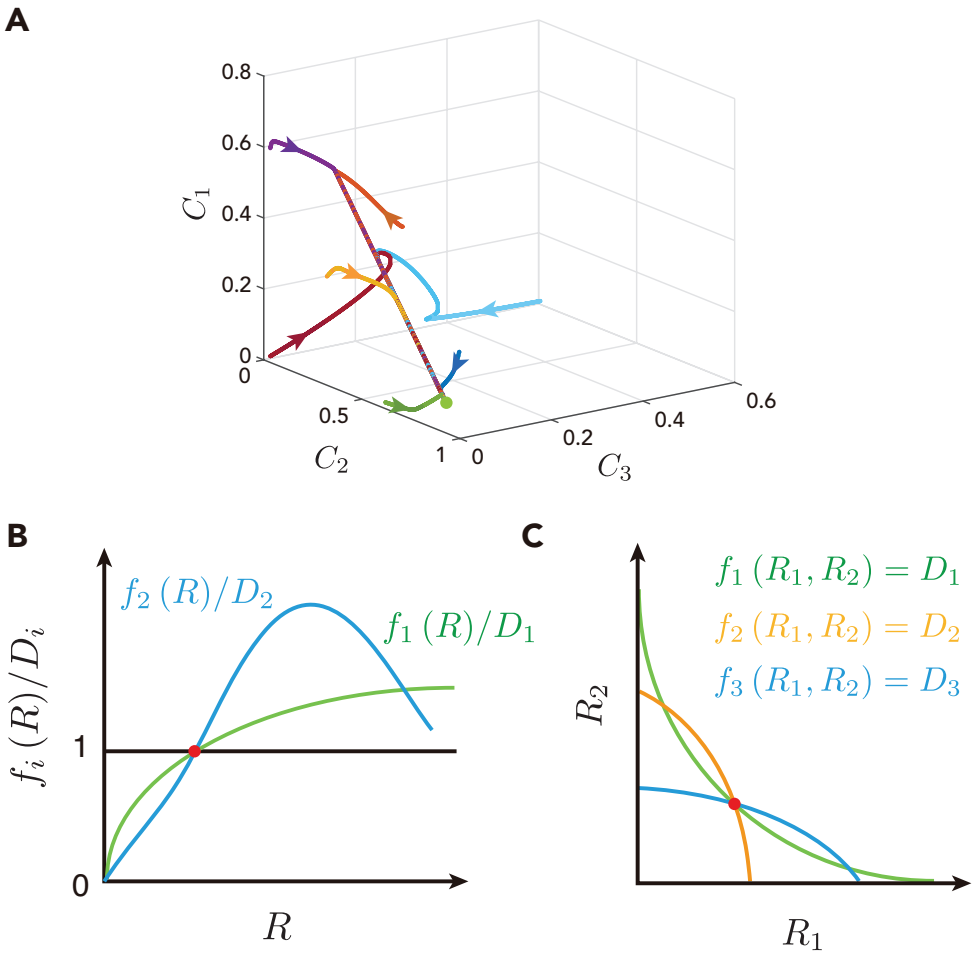

Figure S2: Within the framework of the classical proof, the types of consumer species in steady coexistence cannot more than that of resources except for special parameter cases (Related to Figure 1). **(A)** Representative phase portrait of the trajectories. $M = 3$ and $N = 2$. Two consumer species, at most, can coexist at steady state. Here equations are that shown in Equation 2 where $f_i(R_1, R_2) = \alpha_i^{(1)} R_1 + \alpha_i^{(2)} R_2$ (i =1, 2, 3); $g_j(R_1, R_2, C_1, C_2, C_3) = R_j \left(r_j^{(0)} - \beta_j^{(0)} R_j - \beta_j^{(1)} C_1 - \beta_j^{(2)} C_2 - \beta_j^{(3)} C_3 \right)$ (j=1, 2); $D_1 = 0.0006$; $D_2 = 0.0005$; $D_3 = 0.0004$; $\alpha_1^{(1)} = 0.0013$; $\alpha_2^{(1)} = 0.0011$; $\alpha_1^{(2)} = 0.001$; $\alpha_2^{(2)} = 0.0009$; $r_1^{(0)} = 1.01$; $r_2^{(0)} = 1$; $\beta_1^{(0)} = \beta_2^{(0)} = 1$, $\beta_1^{(1)} = 1.3$; $\beta_2^{(1)} = 1$; $\beta_1^{(2)} = 1.1$; $\beta_2^{(2)} = 0.9$; $\alpha_3^{(1)} = 0.0001$; $\alpha_3^{(2)} = 0.0021$; $\beta_1^{(3)} = 0.1$ and $\beta_2^{(3)} = 2.1$. In the initial condition, $R_1 = 0.01$ and $R_2 = 0.01$ for all trajectories. Finally, all trajectories converge at the green point with $C_1 = 0$. **(B-C)** Special cases permit $M > N$ at steady state. **(B)** $M = 2$ and $N = 1$. **(C)** $M = 3$ and $N = 2$. It is possible that $M > N$ at steady state for a special parameter set (with Lebesgue measure zero), which corresponds to the case that three lines accidentally intersect at a common point (red point in **(B-C)**). A simple scheme of this special case is $f_i = f$, $D_i = D$ (i=1-M).

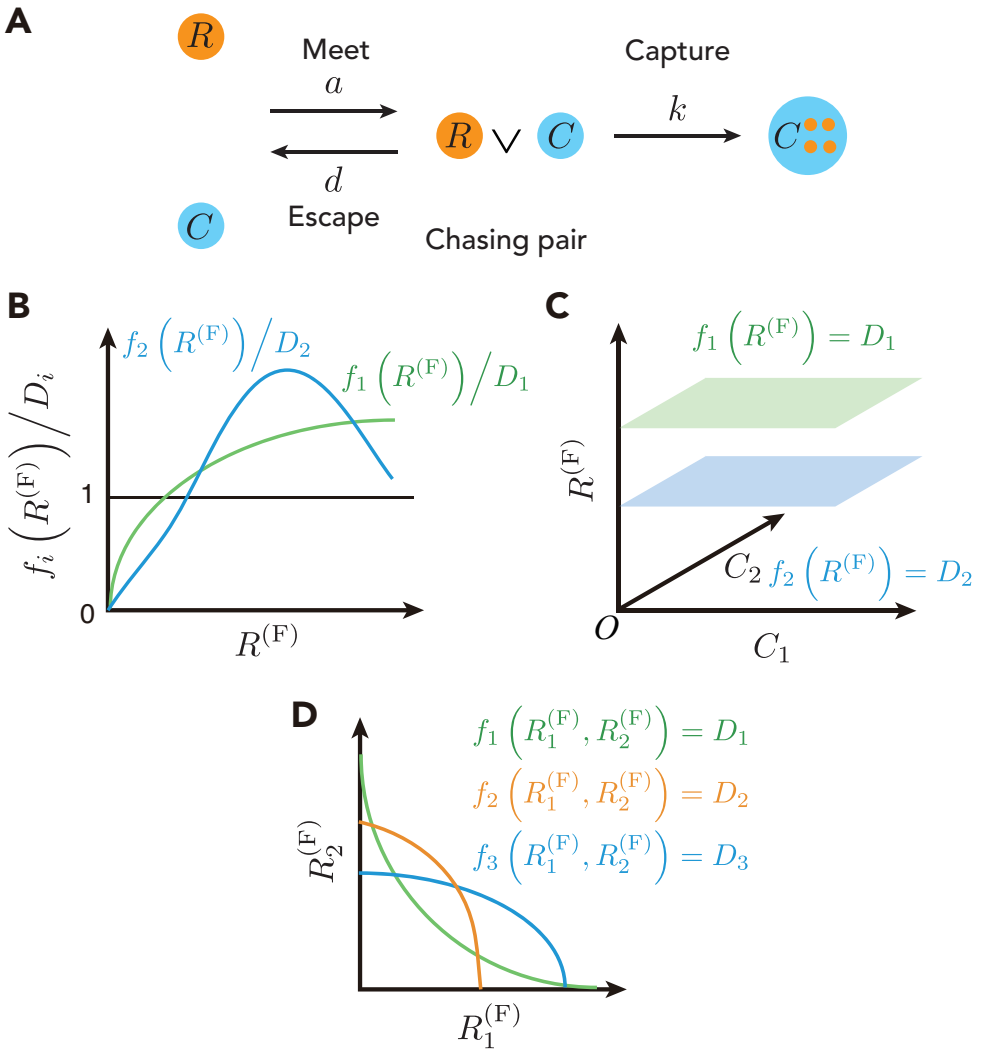

Figure S3: Chasing-pair scenario is still under the constraint of competitive exclusion (Related to Figure 2).

(A) Schematic of the consumption process between consumers and resources. $M = 1$ and $N = 1$. Here a is the encounter rate between a consumer and a resource to form a chasing pair; d is the escape rate of a resource out of a chasing pair; k is the capture rate of consumers in a chasing pair. **(B)** $M = 2$ and $N = 1$. If all consumer species coexist at steady state, $f_i\left(R^{(\mathrm{F})}\right)/D_i = 1$ (i=1, 2). This requires that three lines $y = f_i(R)/D_i$ (i=1, 2) and $y = 1$ share a common point, which normally cannot happen. **(C)** $M = 2$ and $N = 1$. The green plane is parallel to the blue one, and hence they do not have a common point. **(D)** $M = 3$ and $N = 2$. At steady state, if all consumer species coexist, then $f_i\left(R_1^{(\mathrm{F})}, R_2^{(\mathrm{F})}\right) = D_i$ (i=1-3). But three lines normally do not intersect at a common point.

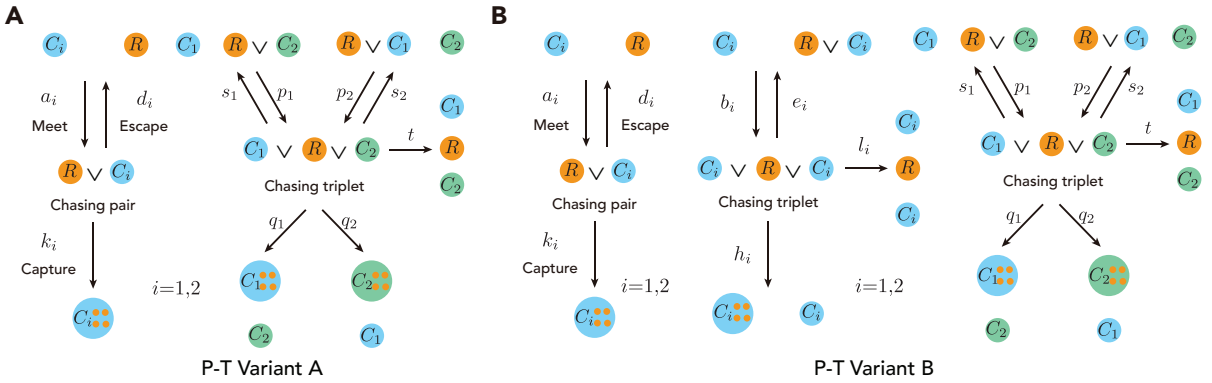

Figure S4: Variants of P-T Model (Related to Figure 2).
(A) P-T Variant A, scenarios involving both chasing pairs and triplets. A triplet consists of two consumers of the same species and a resource (denote as hetero chasing triplet). **(B)** P-T Variant B, scenarios involving both chasing pairs and triplets. A triplet consists of two consumers of the same (denote as homo chasing triplet) or different species and a resource. In **(A-B)**: a_i is the encounter rate between a consumer and a resource to form a chasing pair, d_i is the escape rate of a resource out of a chasing pair, k_i is the capture rate of consumers in a chasing pair; while p_i is the encounter rate between a consumer and an existing chasing pair to form a hetero chasing triplet, s_i and t are the escape rates of a consumer out of a hetero chasing triplet, q_i is the capture rate of consumers in a hetero chasing triplet. In **(B)**: b_i is the encounter rate in forming a homo chasing triplet; e_i and l_i are the escape rates of a consumer out of a homo chasing triplet; h_i is the capture rate of consumer in a homo chasing triplet.

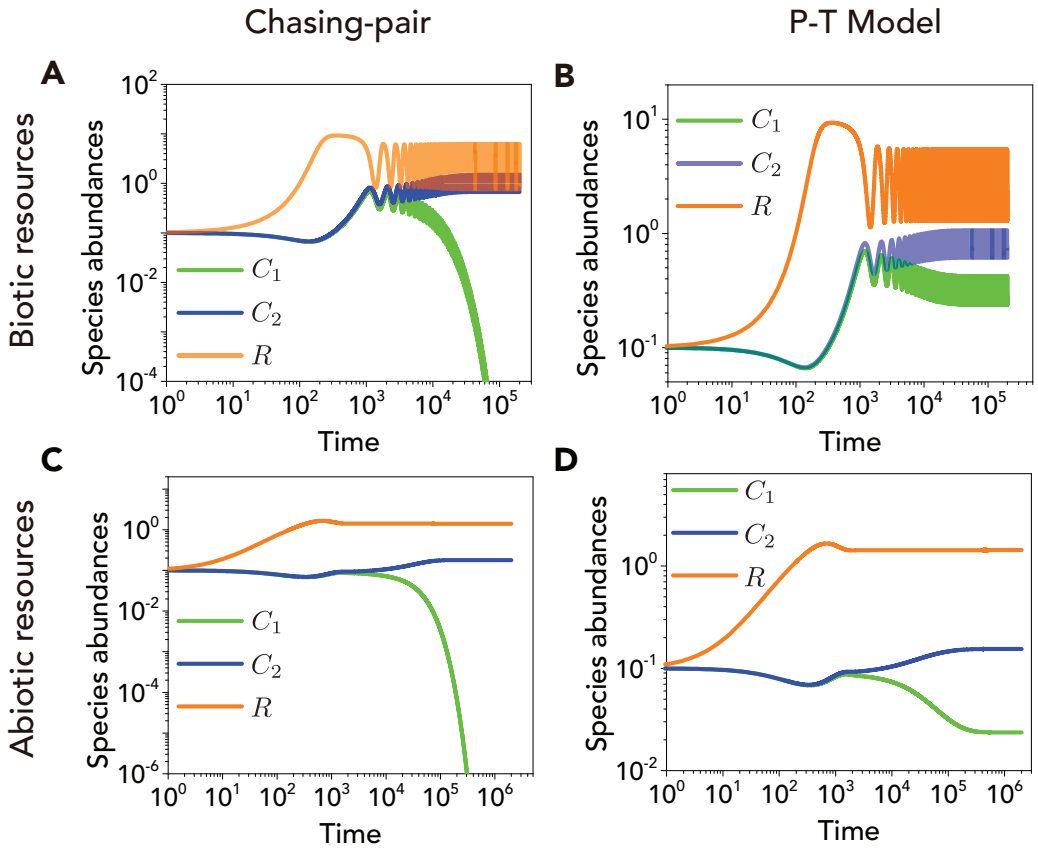

Figure S5: Time course of the abundance of two consumer species (M=2) and one resource species (N=1) (Related to Figure 2).
(A) In the presence of only chasing pairs, only one type of consumer species exists for long, the oscillating dynamics resembles that of the classical predator-prey models (May, 1972). **(B)** In P-T Model (the presence of chasing pairs and triplets), two consumer species coexist at oscillating abundances. **(C)** In the presence of only chasing pairs, consumer species cannot coexist at steady state. **(D)** In P-T Model, both consumer species coexist at steady state. **(A-B)** Biotic resources, **(C-D)** Abiotic resources. **(A)** was simulated from Equation 3, where $g = RR_0(1 - R/K_0) - (k_1x_1 + k_2x_2)$; **(B)** was simulated from Equations 4-5; **(C)** was simulated from Equation 3, where $g = R_a(1 - R/K_0) - (k_1x_1 + k_2x_2)$; (d) was simulated from Equations 4-5. In **(A-D)**: $a_i = 0.1$, $d_i = 0.1$, $k_i = 0.1$, $w_i = 0.1$ (i=1, 2); the initial abundances of (R, C_1, C_2) are $(0.1, 0.1, 0.1)$. In **(A-B)**: $D_2 = 0.005$, $K_0 = 10$, $R_0 = 0.03$, $D_1 = 1.03D_2$. In **(C-D)**: $D_2 = 0.004$, $K_0 = 5$, $R_a = 0.01$, $D_1 = 1.01D_2$. In **(B)** and **(D)**: $b_i = 0.1$, $e_i = 0.1$, $h_i = 0.1$, $l_i = 0.1$ (i=1, 2).

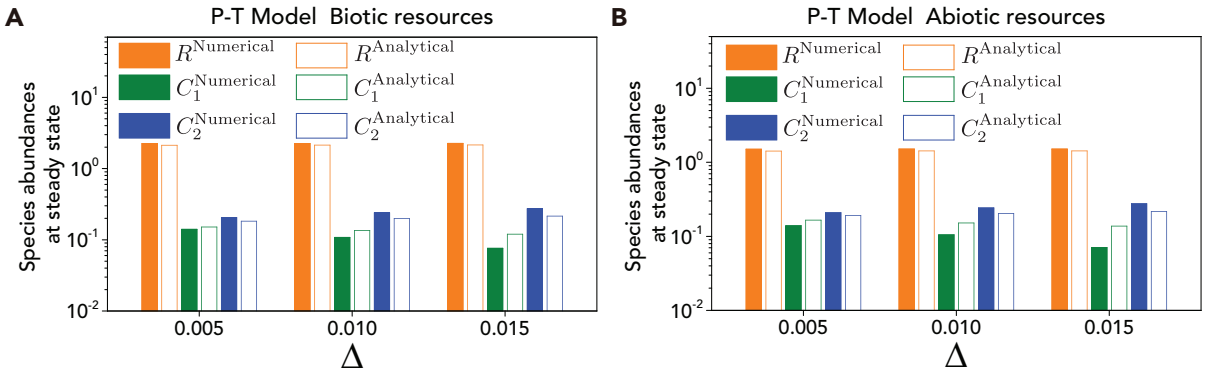

Figure S6: Comparison between analytical solutions and numerical results for the steady-state species abundances in P-T Model (Related to Figure 2).
Color bars are numerical results while hollow bars are analytical solutions. **(A)** biotic resources; **(B)** abiotic resources. **(A-B)** the numerical results (labeled with superscript 'Numerical') were calculated from Equations 4-5, while the analytical results (labeled with superscript 'Analytical') were calculated from Equations S30-S32. In **(A-B)**: $\Delta \equiv (D_1 - D_2)/D_2$, $a_i = 0.1$, $d_i = 0.1$, $k_i = 0.1$, $b_i = 0.1$, $e_i = 0.1$, $h_i = 0.1$, $l_i = 0.1$, $w_i = 0.1$ (i=1, 2). In **(A)**: $D_2 = 0.005$, $K_0 = 10$, $R_0 = 0.01$. In **(B)**: $D_2 = 0.004$, $K_0 = 5$, $R_a = 0.02$.

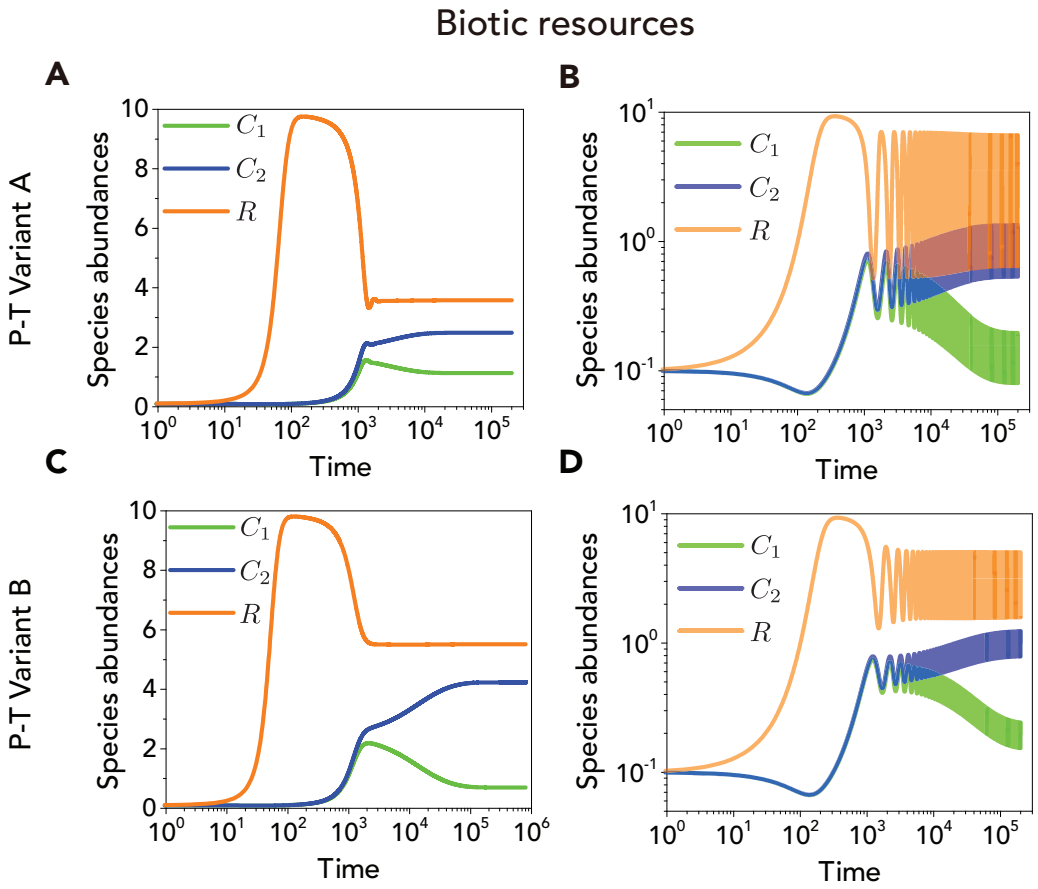

Figure S7: Time course of the abundance of two consumer species (M=2) and one biotic resource species (N=1) (Related to Figures 2, S4).
In the presence of chasing pairs and chasing triplets, two consumer species coexist at steady state (**(A)**, **(C)**) or with oscillating abundances (**(B)**, **(D)**). **(A-B)** P-T Variant A. **(C-D)** P-T Variant B. **(A-B)** were simulated from Equations S34-S35; **(C-D)** were simulated from Equations S36-S37; In **(A-D)**: $a_i = p_i = 0.1$, $d_i = s_i = t = 0.1$, $k_i = 0.1$, $w_i = 0.1$ (i=1, 2); $D_2 = 0.005$, $K_0 = 10$, the initial abundances of (R, C_1, C_2) are $(0.1, 0.1, 0.1)$. In **(A)**: $R_0 = 0.08$, $D_1 = 1.05D_2$, $q_i = 0.1$ (i=1, 2); In **(B)**: $R_0 = 0.03$, $D_1 = 1.02D_2$, $q_i = 0.1$ (i=1, 2); In **(C-D)**: $q_i = 0.05$, $b_i = 0.1$, $e_i = l_i = 0.1$, $h_i = 0.1$ (i=1, 2); In **(C)**: $R_0 = 0.1$, $D_1 = 1.02D_2$; In **(D)**: $R_0 = 0.03$, $D_1 = 1.01D_2$.

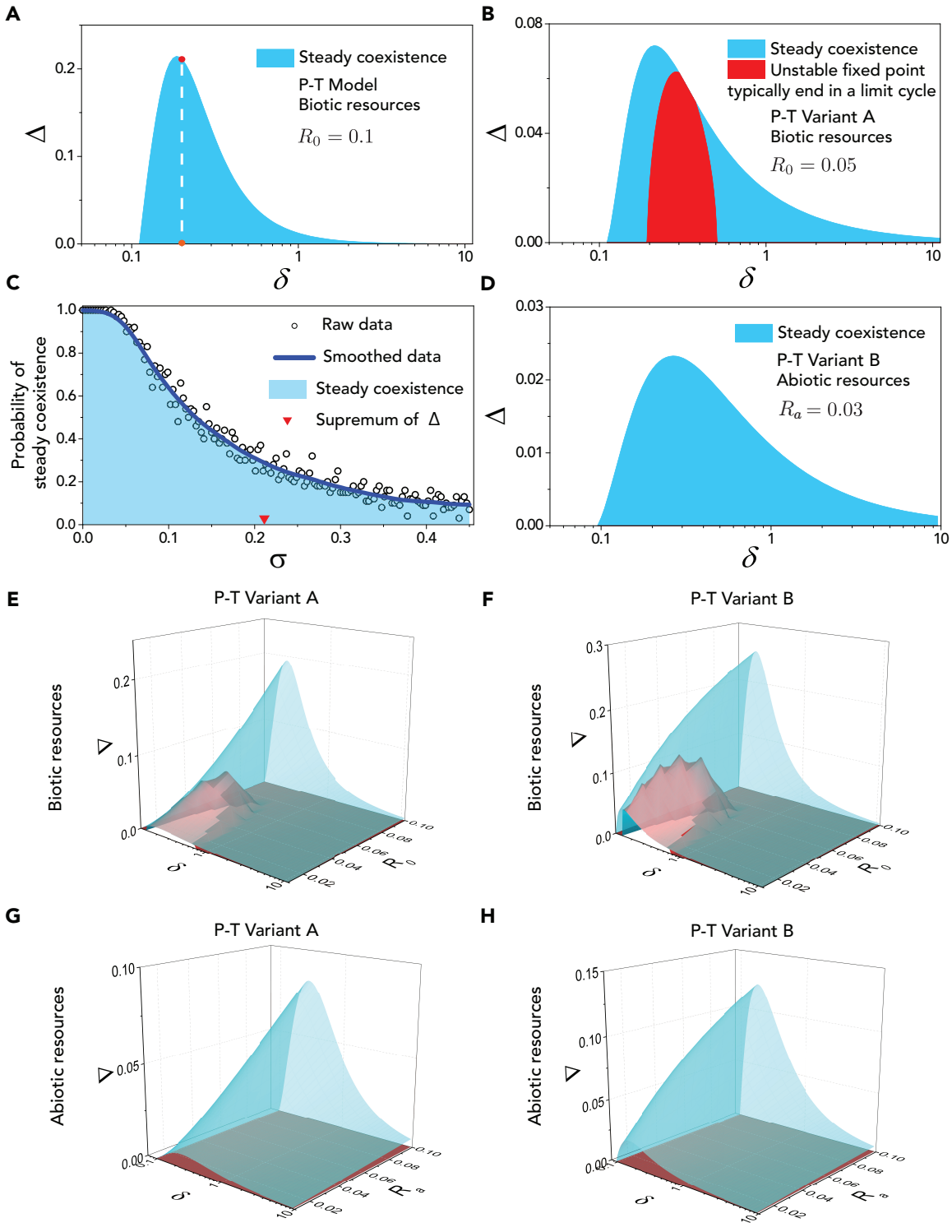

Figure S8: Stable coexistence region of two consumer species competing for one type of resources (Related to Figures 2-3, S4).

Figure S8 *(previous page)*: In **(A-B)**, **(D)** and **(E-H)**, D_i (i=1, 2) is the only different parameter between consumer species C_1 and C_2, and $\Delta \equiv (D_1 - D_2)/D_2$, the relative difference in mortality rate, measures the competitive differences between the two consumer species. δ is a dimensionless multiplier that to tune the capture rate and escape rate parameters for the two-consumer species in each scenario. **(A-B)**, **(D)** The region of stable coexistence (shown in blue, for globally attracting fixed point) for parameter set. **(A)** P-T Model, biotic resource. Parameter values at the orange dot ($\delta = 0.2$) is used in calculating all results shown in (c), red dot marks the upper bound of Δ ($\delta = 0.2$) that permits species coexistence. **(B)** P-T Variant A, biotic resource. Red region corresponds to unstable fixed point, which typically ends in a limit cycle (oscillating time series). **(C)** Probability of steady coexistence for random parameters. First, we chose all parameter exactly the same for two consumer species: $K_0 = 10$, $D_i = 0.005$, $a_i = b_i = 0.1$, $k_i = h_i = 0.1$, $d_i = e_i = l_i = 0.1$, $w_i = 0.1$, $R_0 = 0.1$ ($i = 1, 2$). Then, each parameter except K_0, D_2 (two reduceable parameters, see Sec.VII for details) was multiplied by a random number following normal distribution $\mathcal{N}(1, \sigma^2)$. All the dots are the raw simulation data (from a sample size of 100), while the line are smoothed data over 25 dots. The blue region corresponds to steady coexistence in the samplings. The inverted red triangle marks the supremum of Δ in **(A)**. **(D)**) P-T Variant B, abiotic resource. **(E-H)** Parameters space below the blue surface and above the red surface (in z-axis, for values of Δ) is the stable coexistence region of each case. Parameters space below the red surface is the unstable fixed-point region, which typically ends in a limit cycle. **(E-F)** Cases of Biotic resources. **(G-H)** Cases of abiotic resources. **(E)**, **(G)** Results of P-T Variant A. **(F)**, **(H)** Results of P-T Variant B. **(A)** and **(C)** were calculated from Equations 4-5; **(B)**, **(E)** and **(G)** were calculated from Equations S34-S35; **(D)**, **(F)** and **(H)** were calculated from Equations S36-S37. In **(A-B)**, **(D)** and **(E-H)**, we choose the initial set of parameter values for capture rates and escape rates wherever applicable as follows: $k_i^{(0)} = h_i^{(0)} = q_i^{(0)} = 0.5$, $d_i^{(0)} = e_i^{(0)} = l_i^{(0)} = s_i^{(0)} = t^{(0)} = 0.5$ ($i = 1, 2$), and then tune those parameters with the multiplier δ as follows: $k_i = \delta k_i^{(0)}$, $h_i = \delta h_i^{(0)}$, $q_i = \delta q_i^{(0)}$, $d_i = \delta d_i^{(0)}$, $e_i = \delta e_i^{(0)}$, $l_i = \delta l_i^{(0)}$, $s_i = \delta s_i^{(0)}$, $t = \delta t^{(0)}$ ($i = 1, 2$), and we choose $a_i = b_i = p_i = 0.1$, $w_i = 0.1$ (i=1, 2) wherever applicable. For other parameters, in **(A-B)** and **(E-F)**, $D_2 = 0.005$, $K_0 = 10$; in **(D)** and **(G-H)**, $D_2 = 0.004$, $K_0 = 5$; in **(A)**, $R_0 = 0.1$; in **(B)**, $R_0 = 0.05$; in **(D)**, $R_a = 0.03$.

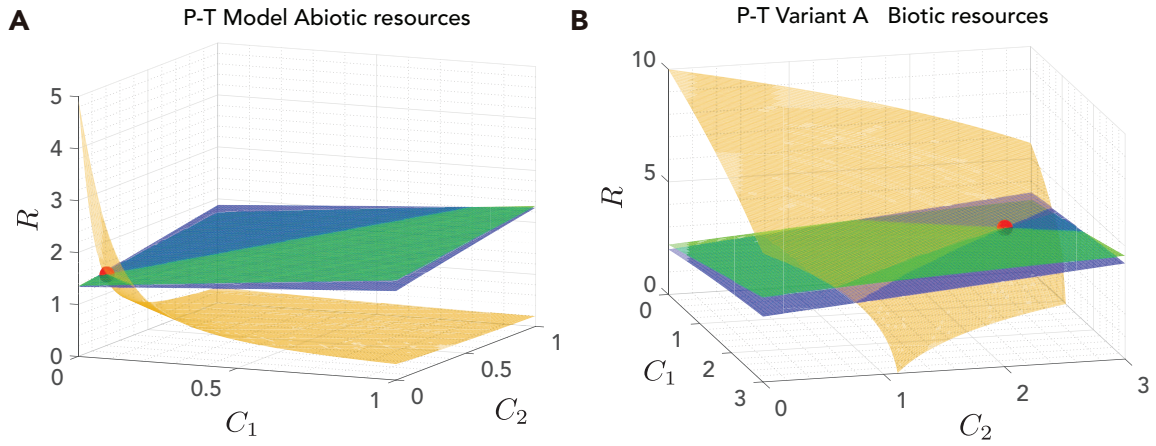

Figure S9: Demonstration of the intuitive explanation with numerical solutions (Related to Figures 2, 4, S4-S5, S7).

(A) In P-T Model (with chasing pairs and triplets) of abiotic resources, numerical solutions confirm that the yellow, green and blue surfaces are not parallel to each other and definitely can have a common point (marked with red dot, see Figure S5D for time series). **(B)** Numerical solutions of P-T Variant A (see Figure S7A for time series). (a) was calculated using Equations 4-5; (b) was calculated from Equations S34-S35. In **(A)**: $a_i = b_i = 0.1$, $d_i = e_i = l_i = 0.1$, $k_i = h_i = 0.1$, $w_i = 0.1$ (i=1, 2); $D_2 = 0.004$, $K_0 = 5$, $R_a = 0.01$, $D_1 = 1.01D_2$. In **(B)**: $a_i = 0.1$, $d_i = 0.1$, $k_i = 0.1$, $w_i = 0.1$,$p_i = 0.1$, $s_i = 0.1$, $q_i = 0.1$ (i=1, 2); $D_1 = 1.05D_2$, $D_2 = 0.005$, $K_0 = 10$,$t = 0.1$, $R_0 = 0.08$.

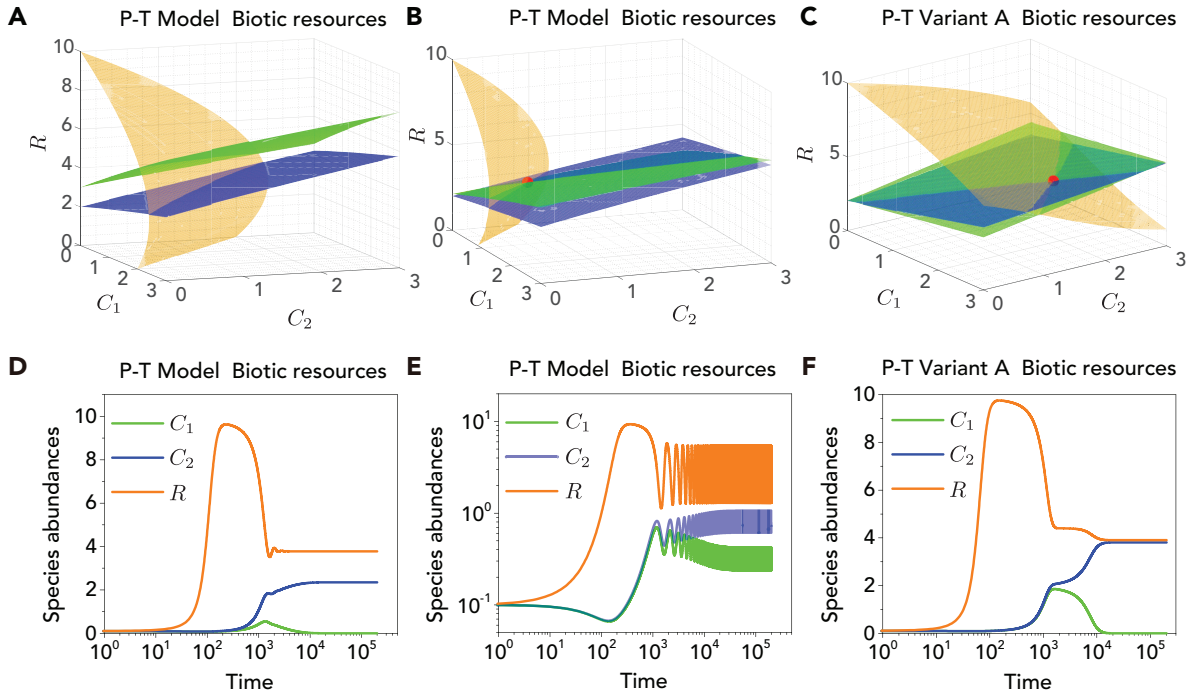

Figure S10: Forming chasing pairs and triplets is not a guarantee for breaking CEP (Related to Figures 2, 4, S4).

(A-C) 3-D demonstration with numerical solutions. **(D-F)** Time course of the abundance of two consumer species (M=2) and one biotic resource species (N=1). **(A)** Although the green surface and blue surface are not parallel to each other, yet they do not have an intersection curve in the first quadrant (i.e., $R, C_1, C_2 > 0$), see **(D)** for time series. **(B)** The intersection point (red dot) of the three surfaces is unstable. All trajectories end in a limit cycle (Figure 3D), see **(E)** (the same as Figure S5B) for time series. **(C)** The intersection point (red dot) of the three surface is unstable, see **(F)** for time series. **(A-B)**, **(D)** and **(E)** were calculated from Equations 4-5; **(C)** and **(F)** were calculated from Equations S34-S35. In **(A-F)**: $a_i = 0.1$, $d_i = 0.1$, $k_i = 0.1$, $w_i = 0.1$ (i=1, 2); $D_2 = 0.005$, $K_0 = 10$. In **(A-B)**, **(D)** and **(E)**: $b_i = 0.1$, $e_i = 0.1$, $h_i = 0.1$, $l_i = 0.1$ (i=1, 2). In **(A)** and **(D)**: $R_0 = 0.05$, $D_1 = 1.2D_2$. In **(B)** and **(E)**: $R_0 = 0.03$, $D_1 = 1.03D_2$. In **(C)** and **(F)** $p_i = 0.1$, $s_i = 0.1$ (i=1, 2); $t = 0.1$, $R_0 = 0.08$, $D_1 = 1.01D_2$, $q_i = 0.05$ (i=1, 2). In **(D-F)**: the initial abundances of (R, C_1, C_2) are $(0.1, 0.1, 0.1)$.

Supplemental Tables

Table S1: Simulation details of the main text Figures (Related to Figures 1-4).

In Figure 1
In Figure 1C, $\alpha = \beta^{(0)} = \beta^{(1)} = \beta^{(1)} = \beta^{(2)} = 1$, $D_1 = 0.0006$ and $D_2 = 0.0005$. All trajectories start with $R = 0.01$. In Figure 1F, $D_1 = 0.0006$, $D_2 = 0.0005$, $D_3 = 0.0004$, $\alpha_1^{(1)} = 0.0013$, $\alpha_2^{(1)} = 0.0011$, $\alpha_1^{(2)} = 0.001$, $\alpha_2^{(2)} = 0.0009$, $r_1^{(0)} = 1.01$, $r_2^{(0)} = 1$, $\beta_1^{(0)} = \beta_2^{(0)} = 1$, $\beta_1^{(1)} = 1.3$, $\beta_2^{(1)} = 1$, $\beta_1^{(2)} = 1.1$, $\beta_2^{(2)} = 0.9$, $\alpha_3^{(1)} = 0.0009$, $\alpha_3^{(2)} = 0.0013$, $\beta_1^{(3)} = 0.9$ and $\beta_2^{(3)} = 1.3$. For the initial condition, we set $R_1 = 0.01$ and $R_2 = 0.01$ for all trajectories.
In Figure 2
In Figures 2C-F: $D_2 = 0.005$, $K_0 = 10$, $a_i = 0.1$, $d_i = 0.1$, $k_i = 0.1$ (i=1, 2); the initial abundances of (R, C_1, C_2) are $(0.1, 0.1, 0.1)$. In Figures 2C-D: $R_0 = 0.05$, $D_1 = 1.08D_2$, $w_i = 0.1$ (i=1, 2). In Figures 2E-F: $R_0 = 0.01$, $D_1 = 1.01D_2$, $w_i = 0.08$ (i=1, 2). In Figures 2D and F: $b_i = 0.1$, $e_i = 0.1$, $h_i = 0.1$, $l_i = 0.1$ (i=1, 2).
In Figure 3
In Figures 3A-D: $a_i = 0.1$, $d_i = 0.1$, $k_i = 0.1$, $b_i = 0.1$, $e_i = 0.1$, $h_i = 0.1$, $l_i = 0.1$, $w_i = 0.1$ (i=1, 2). In Figures 3A, C-D: $w_i = 0.1$ (i=1, 2). In Figure 3A: $R_a = 0.01$, $K_0 = 5$, $D_2 = 0.004$, $D_1 = 1.01D_2$. In Figures 3B-D: $K_0 = 10$, $D_2 = 0.005$. In Figure 3B: $R_0 = 0.01$, $D_1 = 1.01D_2$, $w_i = 0.08$ (i=1, 2). In Figure 3C: $R_0 = 0.08$, $D_1 = 1.08D_2$. In Figure 3D: $R_0 = 0.03$, $D_1 = 1.03D_2$. In Figures 3E-F, we choose the initial set of parameter values for capture rates and escape rates as follows: $k_i^{(0)} = h_i^{(0)} = 0.5$, $d_i^{(0)} = e_i^{(0)} = l_i^{(0)} = 0.5$ ($i = 1, 2$), and then tune those parameters with the multiplier δ as follows: $k_i = \delta k_i^{(0)}$, $h_i = \delta h_i^{(0)}$, $d_i = \delta d_i^{(0)}$, $e_i = \delta e_i^{(0)}$, $l_i = \delta l_i^{(0)}$, ($i = 1, 2$), and we choose $a_i = b_i = 0.1$, $w_i = 0.1$ (i=1, 2). In Figures 3G-H, we choose the initial value of h_i, the capture rate in the chasing triplet: $h_i^{(0)} = 0.1$, and then tune this parameter (and only this parameter) with the multiplier η:$h_i = \eta h_i^{(0)}$, and we choose $a_i = b_i = 0.1$, $k_i = h_i^{(0)} = 0.1$, $d_i = e_i = l_i = 0.1$, $w_i = 0.1$ (i=1, 2). In Figures 3E, G: $D_2 = 0.005$, $K_0 = 10$. In Figures 3F, H: $D_2 = 0.004$, $K_0 = 5$.
In Figure 4
In Figures 4D-E: $a_i = 0.1$, $d_i = 0.1$, $k_i = 0.1$, $w_i = 0.1$ (i=1, 2); $D_2 = 0.005$, $K_0 = 10$. In Figure 4D: $R_0 = 0.05$, $D_1 = 1.3D_2$. In Figure 4E: $b_i = 0.1$, $e_i = 0.1$, $h_i = 0.1$, $l_i = 0.1$ (i=1, 2); $R_0 = 0.05$, $D_1 = 1.08D_2$.

Transparent Methods

I Different forms of the Competitive Exclusion Principle (CEP).

A The earliest form.

The earliest form of the CEP (Volterra, 1928, Gause, 1934, Hardin, 1960), or Gause's law, states that complete competitors cannot coexist, meaning that a more advantageous species can dominate a niche over other species. This was explained in Garret Hardin's classical paper (Hardin, 1960) and manifested in Darwin's fitness survival (Darwin, 1859): supposing that one species owns a doubling rate of 1.01 while another species owns a doubling rate of 1, mathematically, it is easy to find that $\lim_{t\to\infty}\frac{2^t}{2^{1.01t}}=0$, which was interpreted as that a small advantage of one species would ultimately result in extinction of all other competing species (Hardin, 1960).

However, the interpretation above heavily depends on the assumption of exponential growth conditions. Without this assumption, a more advantageous species will not dominate, and coexistence is possible. To illustrate this, here we consider two different scenarios, each contains two types of consumers C_1 and C_2 feeding on two types of resources R_1 and R_2.

1 Microbial ecosystem in a turbidostat.

In a turbidostat, resources R_1 and R_2 (which can be two different types of carbon sources) flow continuously into the system with an adjustable dilution rate $D(t)$ to keep the turbidity (normally the total amount of C_1 and C_2, i.e., $C_{tot}\equiv C_1+C_2$) constant. Here we assume that the growth rate terms of C_i (i=1, 2) follows Holling's type-II functional response (Holling, 1959). The population dynamics can be written as follows:

$$\begin{cases}\dot{R}_1=D(t)\,r_1-D(t)\,R_1-\beta_1^{(1)}\alpha_1^{(1)}C_1\frac{R_1}{R_1+K_1^{(1)}}-\beta_2^{(1)}\alpha_2^{(1)}C_2\frac{R_1}{R_1+K_2^{(1)}}\\ \dot{R}_2=D(t)\,r_2-D(t)\,R_2-\beta_1^{(2)}\alpha_1^{(2)}C_1\frac{R_2}{R_2+K_1^{(2)}}-\beta_2^{(2)}\alpha_2^{(2)}C_2\frac{R_2}{R_2+K_2^{(2)}}\\ \dot{C}_1=\alpha_1^{(1)}C_1\frac{R_1}{R_1+K_1^{(1)}}+\alpha_1^{(2)}C_1\frac{R_2}{R_2+K_1^{(2)}}-D_1C_1-D(t)\,C_1\\ \dot{C}_2=\alpha_2^{(1)}C_2\frac{R_1}{R_1+K_2^{(1)}}+\alpha_2^{(2)}C_2\frac{R_2}{R_2+K_2^{(2)}}-D_2C_2-D(t)\,C_2\end{cases}, \tag{S1}$$

where r_i (i=1, 2) is the quantity of R_i per unit of the flux into the system; D_j (j=1, 2) is the death rate of species C_j, while $\alpha_j^{(i)}$, $\beta_j^{(i)}$ and $K_j^{(i)}$ (i, j=1, 2) are other relevant parameters. Since the turbidity ($C_{tot}\equiv C_1+C_2$) is a constant, consider the case that C_{tot} is very small so that $\beta_j^{(i)}\alpha_j^{(i)}C_i\frac{R_i}{R_i+K_j^{(i)}}\ll D(t)\,R_i$, then $D(t)\,r_i\approx D(t)\,R_i$ (and thus $r_i\approx R_i$), and the population dynamics of C_j follows:

$$\begin{cases}\dot{C}_1=C_1\left(\frac{\alpha_1^{(1)}r_1}{r_1+K_1^{(1)}}+\frac{\alpha_1^{(2)}r_2}{r_2+K_1^{(2)}}-D_1\right)-D(t)\,C_1\\ \dot{C}_2=C_2\left(\frac{\alpha_2^{(1)}r_1}{r_1+K_2^{(1)}}+\frac{\alpha_2^{(2)}r_2}{r_2+K_2^{(2)}}-D_2\right)-D(t)\,C_2\end{cases}. \tag{S2}$$

Note that $\gamma_j\equiv\sum_{i=1,2}\frac{\alpha_j^{(i)}r_i}{r_i+K_j^{(i)}}-D_j$, the effective growth rate of C_j is fixed once parameters $\alpha_j^{(i)}$, $K_j^{(i)}$, r_i and D_j are chosen. Actually, C_j is of exponential growth with effective growth rate γ_j and dilution rate $D(t)$. If $\gamma_1>\gamma_2$, $\lim_{t\to\infty}D(t)=\gamma_1$ and $\lim_{t\to\infty}\frac{C_2(t)}{C_1(t)}=0$, the less competitive species C_2 would ultimately become extinct. Overall, in an idealized turbidostat, an advantageous species outcompetes all other species and dominate the system.

2 Ecosystem in a natural habitat.

We consider a natural system with the population dynamics following the classical consumer-resource model (MacArthur, 1970, Chesson, 1990):

$$\begin{cases} \dot{C}_1 = C_1\left(\alpha_1^{(1)}R_1 + \alpha_1^{(2)}R_2 - D_1\right) \\ \dot{C}_2 = C_2\left(\alpha_2^{(1)}R_1 + \alpha_2^{(2)}R_2 - D_2\right) \\ \dot{R}_1 = g_1\left(R_1\right) - \beta_1^{(1)}\alpha_1^{(1)}C_1R_1 - \beta_2^{(1)}\alpha_2^{(1)}C_2R_1 \\ \dot{R}_2 = g_2\left(R_1\right) - \beta_1^{(2)}\alpha_1^{(2)}C_1R_2 - \beta_2^{(2)}\alpha_2^{(2)}C_2R_2 \end{cases}, \tag{S3}$$

where D_j (j=1, 2) is the death rate of species C_j; $\alpha_j^{(i)}$ and $\beta_j^{(i)}$ (i, j=1,2) are other relevant parameters. $g_i\left(R_i\right)$ (i=1, 2) is the influx of R_i into the system, where we consider $g_i\left(R_i\right) = c_i$ when R_i is abiotic (Posfai et al., 2017) (denote as case A) and $g_i\left(R_i\right) = R_i\left[r_i - R_i/K\right]$ (r_i and K_i are parameters) when R_i is biotic (MacArthur, 1970) (denote as case B). In both cases, rather than the advantageous species excludes the other, C_1 and C_2 actually can coexist. To illustrate this, here we consider a simple scheme that C_1 and C_2 only feed on R_1 and R_2, respectively, i.e., $\alpha_1^{(2)} = \alpha_2^{(1)} = 0$. Then

$$\begin{cases} \dot{C}_1 = C_1\left(\alpha_1^{(1)}R_1 - D_1\right) \\ \dot{C}_2 = C_2\left(\alpha_2^{(2)}R_2 - D_2\right) \\ \dot{R}_1 = g_1\left(R_1\right) - \beta_1^{(1)}\alpha_1^{(1)}C_1R_1 \\ \dot{R}_2 = g_2\left(R_1\right) - \beta_2^{(2)}\alpha_2^{(2)}C_2R_2 \end{cases}. \tag{S4}$$

In case A, at steady state, $R_i = D_i/\alpha_i^{(i)}$ (i=1, 2) and $C_i = c_i/\left(\beta_i^{(i)}D_i\right)$. In case B, $R_i = D_i/\alpha_i^{(i)}$ and $C_i = \frac{r_i - D_i/\left(\alpha_i^{(i)}K_i\right)}{\beta_i^{(i)}\alpha_i^{(i)}}$. Since $\alpha_i^{(i)}, \beta_i^{(i)} > 0$, when $r_i > D_i/\left(\alpha_i^{(i)}K_i\right)$, even if $\alpha_1^{(1)}/D_1 \gg \alpha_2^{(2)}/D_2$ or vice versa, C_1 and C_2 can coexist in both cases A and B.

Generally, in cases described in Equation S3, if $\alpha_1^{(1)}/D_1 > \alpha_2^{(1)}/D_2$, as long as $\alpha_1^{(2)}/D_1 < \alpha_2^{(2)}/D_2$, C_1 and C_2 may coexist. The phenomenon of coexistence can be interpreted as follows: $\alpha_1^{(1)}/D_1 > \alpha_2^{(1)}/D_2$ means that C_1 is more advantageous in the competition for R_1, while $\alpha_1^{(2)}/D_1 < \alpha_2^{(2)}/D_2$ means that C_2 is more advantageous in the competition for R_2. Yet, why C_1 and C_2 can coexist rather the overall advantageous species (the one with larger growth rate) excludes the other?

The underlying reason is that in a long term the growth of C_1 and C_2 in the competition deviate severely from exponential growth. To illustrate this point, we consider the scenario described in Equation S4 ($\alpha_1^{(2)} = \alpha_2^{(1)} = 0$) with a special case that ignoring the death rate ($D_1 = D_2 = 0$). In a long term, $g_i\left(R_i\right) = \beta_i^{(i)}\alpha_i^{(i)}C_iR_i$. In case A, $\dot{C}_i = \frac{g_i(R_i)}{\beta_i^{(i)}} = \frac{c_i}{\beta_i^{(i)}}$, then $C_i\left(t\right) = C_i\left(t=0\right) + \frac{c_i}{\beta_i^{(i)}}t$, and $\lim\limits_{t\to\infty}\frac{C_2(t)}{C_1(t)} = \frac{c_2/\beta_2^{(2)}}{c_1/\beta_1^{(1)}}$, where the consumer populations increase linearly rather than exponentially with time. In case B, $R_i = K_i\left(r_i - \beta_i^{(i)}\alpha_i^{(i)}C_i\right)$ and $\dot{C}_i = \alpha_i^{(i)}K_i\left(r_i - \beta_i^{(i)}\alpha_i^{(i)}C_i\right)C_i$, then $\lim\limits_{t\to\infty}C_i\left(t\right) = r_i/\left(\beta_i^{(i)}\alpha_i^{(i)}\right)$, where the growth of consumer population is limited by the availability of resources. In both cases, both consumer species are not of exponential growth, and clearly, they do coexist.

B The classical form since the 1960s.

Since the 1960s, Robert H. MacArthur and his colleagues (MacArthur and Levins, 1964) formulate the classical form of CEP (MacArthur and Levins, 1964, Levin, 1970, McGehee and Armstrong, 1977): Consider M types of consumer species competing for N types of resources. At steady state the number of coexisting species of consumers cannot exceed that of resources, i.e., $M \geq N$. This classical CEP form stimulates myriads of studies and is the focus of this paper.

II Existing studies.

A Existing mechanisms overcome the limit set by the CEP.

Identifying mechanisms that maintain biodiversity is a central aim in ecology. Various mechanisms (Roy and Chattopadhyay, 2007) have been proposed to overcome the limit set by the CEP and hence explain biodiversity in ecosystems. Those mechanisms can be classified as follows:

a) The ecosystems never reach steady state due to temporal effects of the environment (Hutchinson, 1961, Levins, 1979, Descamps-Julien and Gonzalez, 2005): The relaxation time for the system to reach equilibrium is not short enough compared to the frequency of changes in the environment, such as weather, temperature or seasonal cycle.

b) Spatial heterogeneity or patchiness (Levin, 1974, Richerson et al., 1970): Each local patch obeys CEP, while globally support more species of consumers than resource (because there can be a larger overlap of resource species than that of consumers among different patches).

c) Self-organized dynamics promote biodiversity: when the environment remains constant, biodiversity can naturally emerge when the consumers' densities are intrinsically fluctuating (Koch, 1974, Huisman and Weissing, 1999) or in a chaos (Huisman and Weissing, 1999, Benincà et al., 2008).

d) Special sets of model parameters (with Lebesgue zero-measure): the simplest example for coexistence of unlimited number of consumers is that all species of consumers share the same ratio of hunting rate to death rate (Volterra, 1928). A recent study (Posfai et al., 2017) found that metabolic trade-offs promote diversity at steady state, but the model heavily relies on the assumption that all consumer species share the same death rate.

e) The biodiversity is facilitated by additional factors other than resources: such as cross-feeding (Turner et al., 1996, Goyal and Maslov, 2018, Goldford et al., 2018), toxin (Czárán et al., 2002), rock-paper-scissors relation (Kerr et al., 2002, Kelsic et al., 2015, Grilli et al., 2017), kill the winner (Thingstad and Lignell, 1997), predator interference (Skalski and Gilliam, 2001, Beddington, 1975, Crowley and Martin, 1989, DeAngelis et al., 1975, Kuang et al., 2003), complex interactions (Kelsic et al., 2015, Bairey et al., 2016, Grilli et al., 2017) or co-evolution (Xue and Goldenfeld, 2017).

B GLV models implicitly imply no less resources species than consumers.

We notice that the Generalized Lotka-Volterra (GLV) model is a very popular modeling framework in the study of biodiversity (Rohr et al., 2014). However, we emphasize that the GLV model is within the classical constraint of CEP, because it implicitly assumes more (or at least equal number) species of resources than that of the consumers.

Consider the simplest case of two competing species:

$$\begin{cases} \dot{C}_1 = C_1\left(\alpha_1 - \beta_{11}C_1 - \beta_{12}C_2\right) \\ \dot{C}_2 = C_2\left(\alpha_2 - \beta_{21}C_1 - \beta_{22}C_2\right) \end{cases}. \tag{S5}$$

Here C_i (i=1, 2) stands for the population of consumer species i; α_i denotes the growth rate; β_{ij} (i, j=1, 2) denotes the interaction terms. Generally, in GLV models, there is no specific constraint on coefficients α_i, β_{ij}. To clarify the implicit assumption, we consider a consumer-resource model that is comparable to this case with $M = 2$ and $N = 1$:

$$\begin{cases} \dot{C}_1 = C_1\left(\alpha_1' R - D_1\right) \\ \dot{C}_2 = C_2\left(\alpha_2' R - D_2\right) \\ \dot{R} = g\left(R, C_1, C_2\right) \equiv r_R R\left[r_0\left(1 - R/r_0\right) - \beta_1' C_1 - \beta_2' C_2\right] \end{cases}. \tag{S6}$$

Here, R stands for the population of resources; α_i' (i=1, 2) is the growth rate of consumer species i; D_i denotes the mortality rate; g follows the classical form of MacArthur's consumer-resource model (MacArthur, 1970, Chesson, 1990). By assuming fast equilibrium for the resource species ($\dot{R} = 0$), Equation S6 can be reduced to Equation S5, with $\alpha_i = \alpha_i' r_0 - D_i$, $\beta_{ij} = \alpha_i' \beta_j'$ (i, j=1, 2). Note that there is a strict constraint on coefficients β_{ij}: $\frac{\beta_{11}}{\beta_{12}} = \frac{\beta_{21}}{\beta_{22}}$. With the knowledge of linear algebra (Strang, 1993), it is easy to prove that only when $M \leq N$ can the coefficients in the GLV models be freely chosen.

C Resources involving chemical compounds.

Chemical compounds are generally treated as external factors in CEP studies (Roy and Chattopadhyay, 2007). As shown in Figure S1B, there are $N - N'$ ($N > N'$) types of chemical compounds and N' types of normal resources in the ecosystem, while there are M species of consumers. Essentially, within the classical CEP framework, it is permitted that the coexisting $M > N'$ at steady state as long as $M \leq N$ (except for special cases corresponding to that shown in Figures S2B-C). The proof is same as the schemes shown in Figure 1 of the main text.

III Consumption kinetics.

A Functional form of consumption kinetics

Consider the simplest scenario of the consumption process, with one type of consumers and one type of resources, i.e., $M = 1$ and $N = 1$ (Figure S3A), and we assume both are biotic (see main text). This resembles the simple form of enzymatic reactions,

$$R^{(\mathrm{F})} + C^{(\mathrm{F})} \underset{d}{\overset{a}{\rightleftarrows}} R^{(\mathrm{P})} \vee C^{(\mathrm{P})} \xrightarrow{k} C^{(\mathrm{F})}(+).$$

Here $C^{(\mathrm{F})}$ and $R^{(\mathrm{F})}$ stand for the populations of consumers and resources that are freely wandering around, respectively. When a consumer meets a resource with encounter rate a, they form a chasing pair $R^{(\mathrm{P})} \vee C^{(\mathrm{P})}$ (for simplicity we denote it as x). The resource can escape with rate d, or be caught and consumed with rate k by the consumer, denoted by $C^{(\mathrm{F})}(+)$, where '$(+)$' means gaining biomass. By assuming that the transformation process from $C^{(\mathrm{F})}(+)$ to $C^{(\mathrm{F})}$ is very fast or consumers can still chase resources when gaining biomass, we count $C^{(\mathrm{F})}(+)$ as $C^{(\mathrm{F})}$. By defining the total number of consumers and resources as $C \equiv C^{(\mathrm{F})} + x$ and $R \equiv R^{(\mathrm{F})} + x$. The population dynamics of the consumers follows:

$$\begin{cases} \dot{C} = wkx - DC \\ \dot{x} = aR^{(\mathrm{F})}C^{(\mathrm{F})} - (d+k)\,x \end{cases}, \tag{S7}$$

where D is the mortality rate of consumers (generally $D \ll a, k, d$), while the consumption kinetics is given by kx. w is a biomass conversion ratio (see Sec.III.B).

At steady state $\dot{x} = 0$, rendering a quadratic equation about x: $R^{(\mathrm{F})}C^{(\mathrm{F})} = (R - x)(C - x) = Kx$, where $K \equiv \frac{k+d}{a}$. By considering $0 \leq x \leq \min(R, C)$, we can easily solve for x:

$$x = \frac{(R + C + K)}{2}\left(1 - \sqrt{1 - \frac{4RC}{(R + C + K)^2}}\right). \tag{S8}$$

Since $\frac{4RC}{(R+C+K)^2} < 1$, then $\sqrt{1 - \frac{4RC}{(R+C+K)^2}} \approx 1 - \frac{2RC}{(R+C+K)^2}$, substituting this into Equation S8, we have $x \approx \frac{RC}{R+C+K}$ and the consumption kinetics can be approximated as (Liu et al., 2015)

$$wkx \approx \frac{wkR}{R + C + K}C. \tag{S9}$$

Basically, $f(R, C) \equiv \frac{wkx(R,C)}{C}$ is the functional response or growth rate function, which is both R and C dependent. The approximated form $f(R, C) \approx \frac{wkR}{R+C+K}$ is similar to the Beddington-DeAngelis functional response (Beddington, 1975, DeAngelis et al., 1975), yet quite different from ratio-dependent predation (Arditi and Ginzburg, 1989, Abrams and Ginzburg, 2000), since K is a positive parameter. When the consumer population is much smaller than that of resource, i.e., $C \ll R$, the consumption kinetics reduces to the canonical Michaelis-Menten form (Nelson and Cox, 2017)

$$wkx \approx \frac{wkR}{R + K}C = f(R)\,C. \tag{S10}$$

Note that the C-dependency in the growth rate function disappear in the above consumption kinetics. This is also consistent with the growth rate function form $f(R)$ used in the classical proof of CEP. However, we emphasize that with C-dependency in the growth rate function $f(R, C)$, the classical proof of CEP does not apply.

B Ephemeral consumption process can influence the population dynamics

For consumer species, the time-scale of consumption process is generally much faster than that of the birth and death processes. How can the consumption process influence the population dynamics? To clarify this, we consider a simple scheme as follows. A consumer individual of species C was born with a mass of m_C^{new}. When its mass increases to a critical value m_C^{birth}, it would immediately give birth to a new individual with mass m_C^{new} and itself owns a mass of m_C^{mother} (the birth process). Due to the conservation of mass, $m_C^{\mathrm{birth}} = m_C^{\mathrm{new}} + m_C^{\mathrm{mother}}$. We use D to denote the mortality rate of consumer species C (the death process). Each time a consumer individual eats up a resource individual (from species R), it gains a incremental mass of m_Δ. Here we still use Figure S7A to describe the consumption process. Denote the total mass of consumer species C as M_C, then the population dynamics of M_C follows: $\dot{M}_C = kxm_\Delta - DM_C$, where $x \equiv R^{(\mathrm{P})} \vee C^{(\mathrm{P})}$ represents the chasing pair. Then, the population dynamics of the system can be described as follows:

$$\begin{cases} \dot{x} = aR^{(\mathrm{F})}C^{(\mathrm{F})} - (d+k)\,x, \\ \dot{C} = wkx - DC, \\ \dot{R} = g\,(R, x, C)\,. \end{cases} \tag{S11}$$

Here, $g\,(R, x, C)$ is a unspecified function. Consumers and resources that are freely wandering around are denoted as $C^{(\mathrm{F})}$ and $R^{(\mathrm{F})}$, respectively. w is a biomass conversion ratio: the reciprocal of the number of resource individuals to be consumed to produce a new-born consumer. Generally speaking, w is of the order of $\frac{m_\Delta}{m_C^{\mathrm{new}}} \ll 1$. From the population dynamics equation of C (in Equation S11), although the kinetic parameters for the consumption process are generically much larger than that of the death process: $a, k, d \gg D$ (i.e., the consumption process is ephemeral), x can be quite comparable to C due to a small w, which means that consumers in a chasing pair take a non-negligible portion of the whole consumer populations. Evidently, this conclusion is valid for potential existing species that the consumption process are not ephemeral compared to the birth and death processes (with the same analysis above). Hence the consumption process can influence the population dynamics, and should be explicitly considered in our modeling framework.

IV Chasing-pair scenario is under the constraint of CEP

Although the classical theory does not apply to the C-dependent function form $f\,(R, C)$, we show below that competitive exclusion principle still holds in the chasing-pair scenario.

First, we consider the case of $M = 2$ and $N = 1$ (Figure 2A).

$$\begin{aligned} R^{(\mathrm{F})} + C_1^{(\mathrm{F})} &\underset{d_1}{\overset{a_1}{\rightleftarrows}} R^{(\mathrm{P})} \vee C_1^{(\mathrm{P})} \xrightarrow{k_1} C_1^{(\mathrm{F})}(+) \\ R^{(\mathrm{F})} + C_2^{(\mathrm{F})} &\underset{d_2}{\overset{a_2}{\rightleftarrows}} R^{(\mathrm{P})} \vee C_2^{(\mathrm{P})} \xrightarrow{k_2} C_2^{(\mathrm{F})}(+) \end{aligned}\ ,$$

where $C_i^{(\mathrm{F})}$ (i=1, 2) stands for consumers, $R_j^{(\mathrm{F})}$ stands for resources, $R^{(\mathrm{P})} \vee C_i^{(\mathrm{P})}$ (defined as x_i) stands for chasing pairs, $C_i^{(\mathrm{F})}(+)$ (counted as $C_i^{(\mathrm{F})}$) stands for consumers that caught and consumed the resources, a_i stands for encounter rates, d_i stands for escape rates, and k_i stands for capture rates. Denote the total population of consumers and resources at each moment as $C_i = C_i^{(\mathrm{F})} + x_i$ (i=1, 2) and $R = R^{(\mathrm{F})} + x_1 + x_2$. The population dynamics of the consumers and resources can be written as follows:

$$\begin{cases} \dot{x_1} = a_1 R^{(\mathrm{F})} C_1^{(\mathrm{F})} - (d_1 + k_1)\,x_1 \\ \dot{x_2} = a_2 R^{(\mathrm{F})} C_2^{(\mathrm{F})} - (d_2 + k_2)\,x_2 \\ \dot{C}_1 = w_1 k_1 x_1 - D_1 C_1 \\ \dot{C}_2 = w_2 k_2 x_2 - D_2 C_2 \\ \dot{R} = g\,(R, x_1, x_2, C_1, C_2) \end{cases}, \tag{S12}$$

where the functional form of $g\,(R, x_1, x_2, C_1, C_2)$ is unspecific, D_1 and D_2 denote the death rate of the two consumer species. w_1 and w_2 are biomass conversion ratios (see Sec.III.B).

At steady state, $\dot{x_i} = 0$, we have

$$x_i = \frac{R^{(\mathrm{F})}}{R^{(\mathrm{F})} + K_i} C_i = f_i\left(R^{(\mathrm{F})}\right) C_i, \tag{S13}$$

with $K_i \equiv \frac{d_i + k_i}{a_i}$ (i=1, 2). Substitute Equation S13 into the third and fourth equations in Equation S12, with steady-state condition $\dot{C}_i = 0$ (i=1, 2), we have

$$\begin{cases} \left(f_1\left(R^{(\mathrm{F})}\right) - D_1\right) C_1 = 0 \\ \left(f_2\left(R^{(\mathrm{F})}\right) - D_2\right) C_2 = 0 \end{cases} . \tag{S14}$$

If all consumers can coexist, $f_i\left(R^{(\mathrm{F})}\right)/D_i = 1$ (i=1, 2). These relations are depicted in a 2-dimensional graph (Figure S3B). Compare Figure S3B with Figure 1B, it is evident that the two types of consumers normally cannot coexist at steady state (except for special cases) for similar reason we discussed in the caption of Figure 1.

Now we consider the case of $M = 3$ and $N = 2$.

$$\begin{array}{l}
R_1^{(\mathrm{F})} + C_1^{(\mathrm{F})} \underset{d_1^{(1)}}{\overset{a_1^{(1)}}{\rightleftarrows}} R_1^{(\mathrm{P})} \vee C_1^{(\mathrm{P})} \xrightarrow{k_1^{(1)}} C_1^{(\mathrm{F})}(+) \\
R_1^{(\mathrm{F})} + C_2^{(\mathrm{F})} \underset{d_2^{(1)}}{\overset{a_2^{(1)}}{\rightleftarrows}} R_1^{(\mathrm{P})} \vee C_2^{(\mathrm{P})} \xrightarrow{k_2^{(1)}} C_2^{(\mathrm{F})}(+) \\
R_1^{(\mathrm{F})} + C_3^{(\mathrm{F})} \underset{d_3^{(1)}}{\overset{a_3^{(1)}}{\rightleftarrows}} R_1^{(\mathrm{P})} \vee C_3^{(\mathrm{P})} \xrightarrow{k_3^{(1)}} C_3^{(\mathrm{F})}(+) \\
R_2^{(\mathrm{F})} + C_1^{(\mathrm{F})} \underset{d_1^{(2)}}{\overset{a_1^{(2)}}{\rightleftarrows}} R_2^{(\mathrm{P})} \vee C_1^{(\mathrm{P})} \xrightarrow{k_1^{(2)}} C_1^{(\mathrm{F})}(+) \\
R_2^{(\mathrm{F})} + C_2^{(\mathrm{F})} \underset{d_2^{(2)}}{\overset{a_2^{(2)}}{\rightleftarrows}} R_2^{(\mathrm{P})} \vee C_2^{(\mathrm{P})} \xrightarrow{k_2^{(2)}} C_2^{(\mathrm{F})}(+) \\
R_2^{(\mathrm{F})} + C_3^{(\mathrm{F})} \underset{d_3^{(2)}}{\overset{a_3^{(2)}}{\rightleftarrows}} R_2^{(\mathrm{P})} \vee C_3^{(\mathrm{P})} \xrightarrow{k_3^{(2)}} C_3^{(\mathrm{F})}(+)
\end{array} ,$$

where $C_i^{(\mathrm{F})}$ (i=1, 2, 3) stands for consumers; $R_j^{(\mathrm{F})}$ (j=1,2) stands for resources; $R_j^{(\mathrm{P})} \vee C_i^{(\mathrm{P})}$ (denoted as $x_i^{(j)}$; i=1-3; j=1,2) stands for chasing pairs; $C_i^{(\mathrm{F})}(+)$ (counted as $C_i^{(\mathrm{F})}$; i =1-3) stands for consumers caught and consumed the resources, $a_i^{(j)}$ stands for encounter rates, $d_i^{(j)}$ stands for escape rates, and $k_i^{(j)}$ stands for capture rates. Denote $R_j = R_j^{(\mathrm{F})} + \sum_{i=1}^{3} x_i^{(j)}$ (j=1, 2) and $C_i = C_i^{(\mathrm{F})} + \sum_{j=1}^{2} x_i^{(j)}$ (i=1-3), the population dynamics can be written as:

$$\begin{cases} \dot{x_i}^{(j)} = a_i^{(j)} R_j^{(\mathrm{F})} C_i^{(\mathrm{F})} - \left(d_i^{(j)} + k_i^{(j)}\right) x_i^{(j)} \\ \dot{C}_i = \sum_{j=1}^{2} w_i^{(j)} k_i^{(j)} x_i^{(j)} - D_i C_i \\ \dot{R}_j = g_j\left(R_1, R_2, C_1, C_2, C_3\right) \end{cases} , \tag{S15}$$

with i=1-3 and j=1, 2. Here the functional form of $g_j\left(R_1, R_2, C_1, C_2, C_3\right)$ (j=1, 2) is unspecific. D_i (i=1-3) denotes the death rate of the three consumer species, $w_i^{(j)}$ are biomass conversion ratios (see Sec.III.B).

At steady state, $\dot{x_i}^{(j)} = 0$, we have

$$\begin{cases} x_i^{(1)} \equiv \frac{R_1^{(\mathrm{F})}}{R_2^{(\mathrm{F})} K_i^{(1)}/K_i^{(2)} + R_1^{(\mathrm{F})} + K_i^{(1)}} C_i \\ x_i^{(2)} \equiv \frac{R_2^{(\mathrm{F})}}{R_1^{(\mathrm{F})} K_i^{(2)}/K_i^{(1)} + R_2^{(\mathrm{F})} + K_i^{(2)}} C_i \end{cases} (i = 1\text{-}3), \tag{S16}$$

where $K_i^{(j)} \equiv \frac{d_i^{(j)}+k_i^{(j)}}{a_i^{(j)}}$ (i=1-3 ; j=1, 2). Hence $\sum_{j=1}^{2} w_i^{(j)} k_i^{(j)} x_i^{(j)} = \left(\frac{w_i^{(1)} k_i^{(1)} R_1^{(\mathrm{F})}}{R_2^{(\mathrm{F})} K_i^{(1)} \big/ K_i^{(2)} + R_1^{(\mathrm{F})} + K_i^{(1)}} + \frac{w_i^{(2)} k_i^{(2)} R_2^{(\mathrm{F})}}{R_1^{(\mathrm{F})} K_i^{(2)} \big/ K_i^{(1)} + R_2^{(\mathrm{F})} + K_i^{(2)}} \right) C_i \equiv f_i \left(R_1^{(\mathrm{F})}, R_2^{(\mathrm{F})} \right) C_i$. Substitute the expression of $\sum_{j=1}^{2} w_i^{(j)} k_i^{(j)} x_i^{(j)}$ into Equation S15, with steady-state condition $\dot{C}_i = 0$ (i=1- 3), we have

$$\begin{cases} \left(f_1 \left(R_1^{(\mathrm{F})}, R_2^{(\mathrm{F})} \right) - D_1 \right) C_1 = 0 \\ \left(f_2 \left(R_1^{(\mathrm{F})}, R_2^{(\mathrm{F})} \right) - D_2 \right) C_2 = 0 \\ \left(f_3 \left(R_1^{(\mathrm{F})}, R_2^{(\mathrm{F})} \right) - D_3 \right) C_3 = 0 \end{cases} . \tag{S17}$$

If all consumers can coexist, $f_i \left(R_1^{(\mathrm{F})}, R_2^{(\mathrm{F})} \right) = D_i$ (i=1-3). These relations are depicted in a plane as shown in Figure S3D. Compare Figure S3D with Figure 1E, it is evident that the three types of consumers normally cannot all coexist (except for special cases).

This method can be extended to general cases of $M > N$, where we can obtain a general set of equations in the form of Equations S14 and S17.

V Forming both chasing pairs and chasing triplets can overcome CEP.

Considering again the consumption process, when a consumer is chasing a resource and forming a chasing pair, other consumers, especially consumers of the same species may join to chase the same resource individual. Consider the case of $M = 2$ and $N = 1$ (Figures 2A-B, we denote the combination of both scenarios as P-T Model), but now two consumers of the same species can chase the same resource, forming a chasing triplet (Figure 2B). The consumption process can be described as follows:

$$\begin{aligned}
&R^{(\mathrm{F})} + C_1^{(\mathrm{F})} \underset{d_1}{\overset{a_1}{\rightleftarrows}} R^{(\mathrm{P})} \vee C_1^{(\mathrm{P})} \xrightarrow{k_1} C_1^{(\mathrm{F})}(+) \\
&R^{(\mathrm{F})} + C_2^{(\mathrm{F})} \underset{d_2}{\overset{a_2}{\rightleftarrows}} R^{(\mathrm{P})} \vee C_2^{(\mathrm{P})} \xrightarrow{k_2} C_2^{(\mathrm{F})}(+) \\
&R^{(\mathrm{P})} \vee C_1^{(\mathrm{P})} + C_1^{(\mathrm{F})} \underset{e_1}{\overset{b_1}{\rightleftarrows}} C_1^{(\mathrm{T})} \vee R^{(\mathrm{T})} \vee C_1^{(\mathrm{T})} \\
&R^{(\mathrm{P})} \vee C_2^{(\mathrm{P})} + C_2^{(\mathrm{F})} \underset{e_2}{\overset{b_2}{\rightleftarrows}} C_2^{(\mathrm{T})} \vee R^{(\mathrm{T})} \vee C_2^{(\mathrm{T})} \quad , \\
&C_1^{(\mathrm{T})} \vee R^{(\mathrm{T})} \vee C_1^{(\mathrm{T})} \xrightarrow{h_1} C_1^{(\mathrm{F})}(+) + C_1^{(\mathrm{F})} \\
&C_2^{(\mathrm{T})} \vee R^{(\mathrm{T})} \vee C_2^{(\mathrm{T})} \xrightarrow{h_2} C_2^{(\mathrm{F})}(+) + C_2^{(\mathrm{F})} \\
&C_1^{(\mathrm{T})} \vee R^{(\mathrm{T})} \vee C_1^{(\mathrm{T})} \xrightarrow{l_1} C_1^{(\mathrm{F})} + C_1^{(\mathrm{F})} + R^{(\mathrm{F})} \\
&C_2^{(\mathrm{T})} \vee R^{(\mathrm{T})} \vee C_2^{(\mathrm{T})} \xrightarrow{l_2} C_2^{(\mathrm{F})} + C_2^{(\mathrm{F})} + R^{(\mathrm{F})}
\end{aligned}$$

where $C_i^{(\mathrm{F})}$ (i=1, 2) and $R^{(\mathrm{F})}$ stand for freely wandering consumers and resources respectively, $R^{(\mathrm{P})} \vee C_i^{(\mathrm{P})}$ (denoted as x_i; i=1, 2) stands for chasing pairs, $C_i^{(\mathrm{T})} \vee R^{(\mathrm{T})} \vee C_i^{(\mathrm{T})}$ (denoted as y_i) stands for chasing triplets, $C_i^{(\mathrm{F})}(+)$ (counted as $C_i^{(\mathrm{F})}$) stands for consumers caught and consumed the resources, and a_i, b_i, d_i, e_i, h_i, k_i and l_i stand for relevant parameters specified in Figures 2A and B. Denote $R =$

$R^{(\mathrm{F})}+\sum_{i=1}^{2}(x_i+y_i)$ and $C_i=C_i^{(\mathrm{F})}+x_i+2y_i$ (i=1, 2), the population dynamics can be written as follows:

$$\begin{cases} \dot{x_1}=a_1R^{(\mathrm{F})}C_1^{(\mathrm{F})}-(d_1+k_1)\,x_1-b_1x_1C_1^{(\mathrm{F})}+e_1y_1 \\ \dot{x_2}=a_2R^{(\mathrm{F})}C_2^{(\mathrm{F})}-(d_2+k_2)\,x_2-b_2x_2C_2^{(\mathrm{F})}+e_2y_2 \\ \dot{y_1}=b_1x_1C_1^{(\mathrm{F})}-(h_1+e_1+l_1)\,y_1 \\ \dot{y_2}=b_2x_2C_2^{(\mathrm{F})}-(h_2+e_2+l_2)\,y_2 \\ \dot{C_1}=w_1(k_1x_1+h_1y_1)-D_1C_1 \\ \dot{C_2}=w_2(k_2x_2+h_2y_2)-D_2C_2 \\ \dot{R}=g'\left(R,x_1,x_2,y_1,y_2,C_1,C_2\right) \end{cases}, \tag{S18}$$

where D_i (i=1, 2) denotes the death rate of the consumer species. At steady state, $\dot{x_i}=0$, $\dot{y_i}=0$ (i=1, 2), we have

$$\begin{cases} a_1R^{(\mathrm{F})}\left(C_1-x_1-2y_1\right)-(d_1+k_1)\,x_1-b_1x_1\left(C_1-x_1-2y_1\right)+e_1y_1=0 \\ a_2R^{(\mathrm{F})}\left(C_2-x_2-2y_2\right)-(d_2+k_2)\,x_2-b_2x_2\left(C_2-x_2-2y_2\right)+e_2y_2=0 \\ b_1x_1\left(C_1-x_1-2y_1\right)-(h_1+e_1+l_1)\,y_1=0 \\ b_2x_2\left(C_2-x_2-2y_2\right)-(h_2+e_2+l_2)\,y_2=0 \end{cases}. \tag{S19}$$

Define

$$\begin{cases} P_1^{(i)}=(2d_i+2k_i-h_i-l_i)\,b_i, \\ P_2^{(i)}=(h_i+e_i+l_i)\,a_i, \\ P_3^{(i)}=(d_i+k_i)/a_i, \\ P_4^{(i)}=(h_i+l_i)\,b_i, \\ P_5^{(i)}=(h_i+l_i)/a_i, \end{cases} \qquad i=1,2. \tag{S20}$$

From Equation S19

$$P_1^{(i)}{x_i}^2+\left[P_2^{(i)}\left(P_3^{(i)}+R^{(\mathrm{F})}\right)+P_4^{(i)}C_1\right]x_i-P_2^{(i)}R^{(\mathrm{F})}C_1=0, \tag{S21}$$

and

$$y_i=\frac{R^{(\mathrm{F})}C_i-\left(P_3^{(i)}+R^{(\mathrm{F})}\right)x_i}{2R^{(\mathrm{F})}+P_5^{(i)}}, \tag{S22}$$

with i=1, 2. When $P_1^{(i)}\neq 0$, note that $0\leq x_i\leq\min\left(C_i,R\right)$, then

$$\begin{cases} x_i=\dfrac{\sqrt{\left[P_2^{(i)}\left(P_3^{(i)}+R^{(\mathrm{F})}\right)+P_4^{(i)}C_i\right]^2+4P_1^{(i)}P_2^{(i)}R^{(\mathrm{F})}C_i}-\left[P_2^{(i)}\left(P_3^{(i)}+R^{(\mathrm{F})}\right)+P_4^{(i)}C_i\right]}{2P_1^{(i)}}\equiv u_i'\left(R^{(\mathrm{F})},C_i\right) \\ y_i=\dfrac{R^{(\mathrm{F})}C_i-\left(P_3^{(i)}+R^{(\mathrm{F})}\right)u_i'\left(R^{(\mathrm{F})},C_i\right)}{2R^{(\mathrm{F})}+P_5^{(i)}}\equiv v_i'\left(R^{(\mathrm{F})},C_i\right) \end{cases} \quad (i=1,2). \tag{S23}$$

Note that $R^{(\mathrm{F})}=R-\sum_{i=1}^{2}(x_i+y_i)$, combined with Equation S19, we get x_i, y_i of the following form:

$$\begin{cases} x_i=u_i\left(R,C_1,C_2\right) \\ y_i=v_i\left(R,C_1,C_2\right) \end{cases} \quad (i=1,2). \tag{S24}$$

Consequently,

$$w_i(k_ix_i+h_iy_i)\equiv\Omega_i'\left(R^{(\mathrm{F})},C_1,C_2\right)\equiv\Omega_i\left(R,C_1,C_2\right)(i=1,2). \tag{S25}$$

Importantly, as long as $b_i\neq 0$ (i=1, 2), there is no existence of such variable $U\equiv U\left(R,C_1,C_2\right)$ that satisfy the equality: $\Theta_i\left(U\left(R,C_1,C_2\right)\right)=\frac{\Omega_i(R,C_1,C_2)}{C_i}$ (where function Θ_i is unspecific, see Sec V.A.2 for details).

At steady state, $\dot{C}_i = 0$ (i=1, 2) and $\dot{R} = 0$. Substituting Equations S24-S25 into Equation S18, we get

$$\begin{cases} \Omega_1(R, C_1, C_2) - D_1 C_1 = 0 \\ \Omega_2(R, C_1, C_2) - D_2 C_2 = 0 \\ g(R, C_1, C_2) = 0 \end{cases}, \tag{S26}$$

where $g(R, C_1, C_2) \equiv g'(R, u_i(R, C_1, C_2), v_i(R, C_1, C_2), C_1, C_2)$.

A Intuitive explanation of why forming both chasing pairs and chasing triplets can break CEP

1 Comparison between the classical case, chasing-pair scenario and chasing pair+triplet scenario

With Equation S26, we can give an intuitive explanation why forming both chasing pairs and chasing triplets may break CEP using the functional forms of population dynamics at steady state. To illustrate how the consumers are liberated from the constraint of CEP in the presence of chasing pairs and chasing triplets, we compare it with the classical proof scenario described in Equation 1 and the chasing-pair scenario described with Equation S12, in the case of $M = 2$ and $N = 1$.

In the classical case (Equation 1), if both consumers can coexist at steady state, $f_i(R)/D_i = 1$ (i=1, 2). Now we depict these relations in a three-dimensional space as shown in Figure 4A, where C_1 is the x-axis, C_2 the y-axis and R the z-axis. The green plane corresponds to $f_1(R)/D_1 = 1$ while the blue plane corresponds to $f_2(R)/D_2 = 1$. Note that in principle there could be multiple green/blue planes if the equation $f_i(R)/D_i = 1$ has multiple solutions. These planes are parallel to the plane $R = 0$ and hence do not share a common point (except for special cases).

In the presence of chasing pairs (Equation S12), if the two consumer species can coexist at steady state, $f_i\left(R^{(\mathrm{F})}\right)/D_i = 1$ (i=1, 2) (Equation S14). On one hand, we can depict these relations in Figure S3C, where C_1 is the x-axis, C_2 the y-axis and $R^{(\mathrm{F})}$ the z-axis. The green plane corresponds to $f_1\left(R^{(\mathrm{F})}\right)/D_1 = 1$ while the blue plane corresponds to $f_2\left(R^{(\mathrm{F})}\right)/D_2 = 1$. Those planes are parallel to the plane $R^{(\mathrm{F})} = 0$, and thus do not share a common point (except for special cases). On the other hand, we can depict the relations in Equation S14 in a coordinate where the z-axis is R rather than $R^{(\mathrm{F})}$. As shown in Figure 4B, the green surface corresponds to $f_1\left(R^{(\mathrm{F})}\right)/D_1 = 1$ while the blue surface corresponds to $f_2\left(R^{(\mathrm{F})}\right)/D_2 = 1$. Essentially, it is a coordinate transformation from Figure S3C. With the knowledge of topology (Kelley, 2017), we know that the green surface is parallel to the blue surface and normally do not share a common point (except for special cases that two surfaces completely overlap).

In the presence of both chasing pairs and chasing triplets, we depict the requirement for coexistence at steady state (Equation S26) in Figure 4C, where C_1 is the x-axis, C_2 the y-axis and R the z-axis. The green surface corresponds to $w_1(R, C_1, C_2) = D_1 C_1$, while the blue surface corresponds to $w_2(R, C_1, C_2) = D_2 C_2$, and the yellow surface corresponds to $g(R, C_1, C_2) = 0$. As determined from Equation S18, the green surface is not parallel to the blue one, and thus they have at least one intersection curve (shown as the dashed purple curve in Figure 4C). Since a curve and a surface can normally have an intersection point, the three surfaces of different colors can normally have at least one intersection point (shown as the red point in Figure 4C). As long as those intersection points locate within the feasible region, i.e., $\min(R, C_1, C_2) > 0$, the two consumer species can coexist at steady state. Numerical results (exact solution) shown in Figures 4D-E and Figure S9 (comparable to Figures 4B-C) confirm our intuitive explanation.

2 Triplets or higher order terms lead to symmetry breaking in the constraint of the CEP

The numerical results shown in Figure 4E and Figure S9 clearly demonstrate that in the presence of both chasing pairs and chasing triplets, the three surfaces that correspond to $\dot{C}_1 = 0$, $\dot{C}_2 = 0$ and $\dot{R} = 0$ are unparallel to each other and can share an intersect point (red points in Figure 4E and Figure S9). This means that in Equation S25, it is impossible for any variable, say $U \equiv U(R, C_1, C_2)$ to satisfy the equality:$\Theta_i(U(R, C_1, C_2)) = \frac{\Omega_i(R, C_1, C_2)}{C_i}$ (where function Θ_i is unspecific). Otherwise, $\Theta_i(U(R, C_1, C_2)) = D_i$ (i=1, 2), the planes that correspond to $\dot{C}_1 = 0$ and $\dot{C}_2 = 0$ are parallel to the C_1-O-C_2 plane (O is the origin point) in the $(C_1, C_2, U(R, C_1, C_2))$ coordinate and corresponds to parallel

surfaces in the (C_1, C_2, R) coordinate. Meanwhile, in the classical case, R corresponds to $U(R, C_1, C_2)$ and in the chasing-pair scenario, $R^{(\mathrm{F})}$ corresponds to $U(R, C_1, C_2)$.

To investigate why there is no existence of $U(R, C_1, C_2)$ in scenario involving both chasing pairs and chasing triplets, we revisit the steady state form of Equation S18. Combined with $C_i = C_i^{(\mathrm{F})} + x_i + 2y_i$ (i=1, 2), then

$$\begin{cases} C_i^{(\mathrm{F})} = \frac{(C_i - x_i)(h_i + e_i + l_i)}{h_i + e_i + l_i + 2b_i x_i}, \\ R^{(\mathrm{F})} = \frac{(d_i + k_i)}{a_i} \frac{x_i(h_i + e_i + l_i + 2b_i x_i)}{(C_i - x_i)(h_i + e_i + l_i)} + \frac{b_i(h_i + l_i)}{a_i(h_i + e_i + l_i)} x_i, \qquad i = 1, 2. \\ y_i = \frac{b_i}{h_i + e_i + l_i} x_i C_i^{(\mathrm{F})} = x_i \frac{b_i(C_i - x_i)}{h_i + e_i + l_i + 2b_i x_i}. \end{cases} \tag{S27}$$

From the last two equations in Equation S27, we find that

$$\begin{cases} x_i = x_i\left(R^{(\mathrm{F})}\right), \\ y_i = y_i\left(R^{(\mathrm{F})}, C_i\right) = x_i\left(R^{(\mathrm{F})}\right) \frac{b_i(C_i - x_i\left(R^{(\mathrm{F})}\right))}{h_i + e_i + l_i + 2b_i x_i\left(R^{(\mathrm{F})}\right)}. \end{cases} \tag{S28}$$

Then

$$\frac{\Omega_i(R, C_1, C_2)}{C_i} = \frac{w_i}{C_i}\left(k_i x_i\left(R^{(\mathrm{F})}\right) + h_i y_i\left(R^{(\mathrm{F})}, C_i\right)\right) \equiv \Theta_i'\left(R^{(\mathrm{F})}, C_i\right), \quad i = 1, 2. \tag{S29}$$

Note that in Equation S29, only when $b_i = 0$, can $\Theta_i'\left(R^{(\mathrm{F})}, C_i\right)$ be reduced to $\Theta_i'\left(R^{(\mathrm{F})}\right)$, otherwise there is no existence of $U(R, C_1, C_2)$. Consequently, the triplet term y_i ($b_i \neq 0$) breaks the symmetric constraint in the equations form, i.e., the existence of $U(R, C_1, C_2)$, which overcomes CEP. Similarly, P-T Variants A-B (see Sec.V.C) or scenarios involving even higher order terms (e.g. quadruplet, quintuplets) are subject to the same analysis above and results in no existence of $U(R, C_1, C_2)$. Actually, chasing pair scenario is a special case of P-T Model when $b_i = 0$, and so does triplet scenario (with chasing pairs) for quadruplet (or quintuplets et.al) scenarios (with chasing pairs and chasing triplets). Thus, the fact that chasing triplet scenario can overcome CEP naturally means that all higher order terms scenarios (triplet or higher) can break CEP. In sum, higher order terms (triplet or higher) lead to symmetry breaking in the constraint of the equation form that overcomes CEP.

B Analytical solutions to steady-state species abundances

Generically, there is no closed form solution to Equation S18. However, when the abundance of resources are much larger than that of consumers, $R \gg C_1, C_2$, which applies to almost all cases in the wild, then $R \approx R^{(\mathrm{F})}$. Combining these results with $\dot{C}_i = 0$ (i=1, 2) and $\dot{g} = 0$,

$$\begin{cases} x_i \approx \frac{\left[P_2^{(i)}\left(P_3^{(i)} + R\right) + P_4^{(i)} C_i\right]}{2P_1^{(i)}} \left\{\sqrt{1 + \frac{4P_1^{(i)} P_2^{(i)} R C_i}{\left[P_2^{(i)}\left(P_3^{(i)} + R\right) + P_4^{(i)} C_i\right]^2}} - 1\right\} \\ y_i \approx \frac{RC_i - \left(P_3^{(i)} + R\right) x_i}{2R + P_5^{(i)}} \end{cases}.$$

Note that $\frac{4P_1^{(i)} P_2^{(i)} R C_i}{\left[P_2^{(i)}\left(P_3^{(i)} + R\right) + P_4^{(i)} C_i\right]^2} \sim \frac{4P_1^{(i)} RC}{P_2^{(i)}\left(P_3^{(i)} + R\right)^2} \sim \frac{C}{R} \ll 1$, where $\sim$ means the same order of magnitude. Then, using the approximation that $\sqrt{1 - x} \approx 1 - x/2$ (when $x \ll 1$),

$$\begin{cases} x_i \approx \frac{P_2^{(i)} R C_i}{P_2^{(i)}\left(P_3^{(i)} + R\right) + P_4^{(i)} C_i} \\ y_i \approx \frac{RC_i}{2R + P_5^{(i)}} \left[\frac{P_4^{(i)} C_i}{P_2^{(i)}\left(P_3^{(i)} + R\right) + P_4^{(i)} C_i}\right] \end{cases}.$$

Basically, the functional response:

$$\begin{aligned} f_i(R, C_1, C_2) &\equiv \frac{w_i(k_i x_i(R, C_1, C_2) + h_i y_i(R, C_1, C_2))}{C_i} \\ &\approx w_i\left(k_i P_2^{(i)} + \frac{h_i P_4^{(i)} C_i}{2R + P_5^{(i)}}\right)\left[\frac{R}{P_2^{(i)}\left(P_3^{(i)} + R\right) + P_4^{(i)} C_i}\right] \end{aligned}$$

depends on both consumer and resource, but not their ratio. Meanwhile, $k_i x_i + h_i y_i = \frac{D_i}{w_i} C_i$, then $\left(k_i P_2^{(i)} + \frac{h_i P_4^{(i)} C_i}{2R + P_5^{(i)}}\right)\left[\frac{R}{P_2^{(i)}\left(P_3^{(i)} + R\right) + P_4^{(i)} C_i}\right] \approx \frac{D_i}{w_i}$, while $\frac{h_i P_4^{(i)} C_i}{\left(2R + P_5^{(i)}\right) k_i P_2^{(i)}} \sim \frac{C_i}{R} \ll 1$. With all these approximation, then

$$C_1 = \frac{P_2^{(1)} R\left(w_1 k_1 / D_1 - 1\right) - P_2^{(1)} P_3^{(1)}}{P_4^{(1)}}, \tag{S30}$$

$$C_2 = \frac{P_2^{(2)} R\left(w_2 k_2 / D_2 - 1\right) - P_2^{(2)} P_3^{(2)}}{P_4^{(2)}}. \tag{S31}$$

We assume that the population dynamics of the resources follow Equations 4-5, then, for biotic resources,

$$R = \frac{\sqrt{{P_6}^2 + 4 P_6 P_7} - P_6}{2}, \tag{S32}$$

where $P_6 \equiv \frac{K_0}{r_0}[\frac{P_2^{(1)}(k_1 - D_1/w_1)}{P_4^{(1)}} + \frac{P_2^{(2)}(k_2 - D_2/w_2)}{P_4^{(2)}} - r_0]$ and $P_7 = \frac{K_0}{r_0}(\frac{D_1}{w_1}\frac{P_2^{(1)} P_3^{(1)}}{P_4^{(1)}} + \frac{D_2}{w_2}\frac{P_2^{(2)} P_3^{(2)}}{P_4^{(2)}})$. For abiotic resources,

$$R = \frac{r_0 + (\frac{D_1}{w_1}\frac{P_2^{(1)} P_3^{(1)}}{P_4^{(1)}} + \frac{D_2}{w_2}\frac{P_2^{(2)} P_3^{(2)}}{P_4^{(2)}})}{\frac{P_2^{(1)}(k - D_1/w_1)}{P_4^{(1)}} + \frac{P_2^{(2)}(k - D_2/w_2)}{P_4^{(2)}} + \frac{r_0}{K_0}}. \tag{S33}$$

Equations S30-S33 are the analytical solutions to the steady-state species abundances under the approximation that $R \gg C_1, C_2$. In Figure 2F, we show the analytical solutions of biotic resource case, which agree well with the simulation results. In Figure S6, we compared the analytical solutions (Equations S30-S33, the approximate solutions) of both the biotic and abiotic resource case to the numerical results (the exact solutions) at steady state, which overall shows good consistency for both cases. Here we assign D_i (i=1, 2) to be the only different parameter between consumer species C_1 and C_2, then $\Delta \equiv (D_1 - D_2)/D_2$, the relative difference in mortality rate, measures the competitive differences between the two consumer species. In Figure S6, we find that the analytical solution is closer to the exact solution when two consumer species are similarly competitive, while it deviates more when the competitive difference between the two consumer species gets larger within the coexistence region (the analytical solution involves approximation). Overall, the analytical solutions (Equations S30-S33) are good approximations to predict species abundances at steady state, while exact solutions are required to identify the boundary of parameter space for species coexistence.

C Scenarios with other chasing triplet forms

To fully take into account scenarios involving different forms of chasing triplet (with the presence of chasing pair), we further consider cases where the chasing triplet is formed between different species of consumers (denoted as P-T Variant A, see Figure S4A) or either between the same or different species (denoted as P-T Variant B, see Figure S4B).

In P-T Variant A (Figure S4A), the population dynamics can be written as follows:

$$\begin{cases} \dot{x_1} = a_1 R^{(\mathrm{F})} C_1^{(\mathrm{F})} - (d_1 + k_1)\, x_1 - p_2 x_1 C_2^{(\mathrm{F})} + s_2 z, \\ \dot{x_2} = a_2 R^{(\mathrm{F})} C_2^{(\mathrm{F})} - (d_2 + k_2)\, x_2 - p_1 x_2 C_1^{(\mathrm{F})} + s_1 z, \\ \dot{z} = p_1 x_2 C_1^{(\mathrm{F})} + p_2 x_1 C_2^{(\mathrm{F})} - (q_1 + q_2 + s_1 + s_2 + t)\, z, \\ \dot{C}_i = w_i(k_i x_i + q_i z) - D_i C_i, \quad i = 1, 2; \\ \dot{R} = g\left(R, x_1, x_2, z, C_1, C_2\right), \end{cases} \tag{S34}$$

where $x_i \equiv R^{(\mathrm{P})} \vee C_i^{(\mathrm{P})}$ represents the chasing pairs, $z \equiv C_1^{(\mathrm{T})} \vee R^{(\mathrm{T})} \vee C_2^{(\mathrm{T})}$ represents the chasing triplets, $C_i^{(\mathrm{F})}$ (i=1, 2) and $R^{(\mathrm{F})}$ stand for freely wandering consumers and resources, respectively. a_i, d_i, k_i, p_i, q_i, s_i and t stand for consuming process relevant parameters specified in the figure captions of Figure S4A. $C_i = C_i^{(\mathrm{F})} + x_i + z$ (i=1, 2) and $R = R^{(\mathrm{F})} + x_1 + x_2 + z$ are the populations of consumers and resources, respectively. D_i represents the mortality rate of the consumer species, w_i is the biomass conversion ratio. Assuming that the dynamics of resources g follows the construction principle as that of

the MacArthur's Model (MacArthur, 1970, Chesson, 1990), we have

$$g\left(R,x_1,x_2,z,C_1,C_2\right) = \begin{cases} RR_0(1-R/K_0)-(k_1x_1+k_2x_2)-(q_1+q_2)z, \\ \qquad\qquad\qquad\qquad \text{for biotic resources.} \\ R_a(1-R/K_0)-(k_1x_1+k_2x_2)-(q_1+q_2)z, \\ \qquad\qquad\qquad\qquad \text{for abiotic resources.} \end{cases} \tag{S35}$$

In P-T Variant B (Figure S4B), the population dynamics can be written as follows:

$$\begin{cases} \dot{x_1} = a_1R^{(\mathrm{F})}C_1^{(\mathrm{F})} - (d_1+k_1)\,x_1 - b_1x_1C_1^{(\mathrm{F})} + e_1y_1 - p_2x_1C_2^{(\mathrm{F})} + s_2z, \\ \dot{x_2} = a_2R^{(\mathrm{F})}C_2^{(\mathrm{F})} - (d_2+k_2)\,x_2 - b_2x_2C_2^{(\mathrm{F})} + e_2y_2 - p_1x_2C_1^{(\mathrm{F})} + s_1z, \\ \dot{y_i} = b_ix_iC_i^{(\mathrm{F})} - (h_i+e_i+l_i)\,y_i, \quad i=1,2, \\ \dot{z} = p_1x_2C_1^{(\mathrm{F})} + p_2x_1C_2^{(\mathrm{F})} - (q_1+q_2+s_1+s_2{+}t)\,z, \\ \dot{C_i} = w_i(k_ix_i+h_iy_i+q_iz) - D_iC_i, \quad i=1,2, \\ \dot{R} = g\left(R,x_1,x_2,y_1,y_2,z,C_1,C_2\right). \end{cases} \tag{S36}$$

where $x_i \equiv R^{(\mathrm{P})} \vee C_i^{(\mathrm{P})}$ represents the chasing pairs, $y_i \equiv C_i^{(\mathrm{T})} \vee R^{(\mathrm{T})} \vee C_i^{(\mathrm{T})}$ and $z \equiv C_1^{(\mathrm{T})} \vee R^{(\mathrm{T})} \vee C_2^{(\mathrm{T})}$ represent the chasing triplets, $C_i^{(\mathrm{F})}$ (i=1, 2) and $R^{(\mathrm{F})}$ stand for freely wandering consumers and resources, respectively. a_i, b_i, d_i, e_i, h_i, k_i, l_i, p_i, q_i, s_i and t stand for consuming process relevant parameters specified in the figure captions of Figure S4B. $C_i = C_i^{(\mathrm{F})} + x_i + 2y_i + z$ (i=1, 2) and $R = R^{(\mathrm{F})} + \sum_{i=1}^{2}(x_i+y_i) + z$ are the populations of consumers and resources, respectively. D_i represents the mortality rate of the consumer species and w_i is the biomass conversion ratio.

Assuming that g follows the construction principle as that of the MacArthur's Model (MacArthur, 1970, Chesson, 1990), we have

$$g\left(R,x_1,x_2,y_1,y_2,z,C_1,C_2\right) = \begin{cases} RR_0(1-R/K_0)-(k_1x_1+h_1y_1)-(k_2x_2+h_2y_2)-(q_1+q_2)z, \\ \qquad\qquad\qquad\qquad \text{for biotic resources.} \\ R_a(1-R/K_0)-(k_1x_1+h_1y_1)-(k_2x_2+h_2y_2)-(q_1+q_2)z,, \\ \qquad\qquad\qquad\qquad \text{for abiotic resources.} \end{cases} \tag{S37}$$

In both P-T Variants, two consumer species can coexist either steadily (Figures S7A, C) or with sustained oscillations (Figures S7B, D) when there is only one type of resource species.

D Non-special parameter space for species coexistence

To figure out if there is a non-zero measure parameter space to facilitate species coexistence, we set D_i (i=1, 2) to be the only different parameter between consumer species C_1 and C_2, and all capture rates and escape rates are multiplied by δ (a dimensionless multiplier) (see Figures S8A, B, D). In all Models (P-T Model and P-T Variants A-B), for a wide range of δ, we find that there is upper bound tolerance for Δ (Figures S8A, B, D), below which there are coexistence solutions for the two consumer species (the colored region). In the case that the resources are abiotic or for some parameters of R_a, the colored region all corresponds to stable coexistence (Figures S8A, D, blue region), while in the case that the resources are biotic, for some other parameters of R_0, there is a region corresponds to unstable fixed point (Figure S8B, red region), which typically ends in a limit cycle. To demonstrate that species coexistence under a non-zero competitive difference (i.e., $\Delta > 0$ when D_i is the only different parameter between two consumer species) really means a non-zero parameter space and the supremum of $\Delta > 0$ actually measures the likelihood for coexistence, we conducted random sampling analysis. Specifically, we first chose all parameter exactly the same for two consumer species (corresponds to the orange dot in Figure S8A). Then, all parameters except K_0, D_2 (two reducible parameters with dimensionless analysis whose values can be set as arbitrary positive values, see Sec.VII for details) are multiplied by a random number following normal distribution $\mathcal{N}(1,\sigma^2)$. Obviously, σ measures the random extent of the

parameter and for each value of σ, we counted the steady coexistence percentage. The probability of steady coexistence for different values of σ is shown in Figure S8C, the inverted red triangle denotes the supremum of Δ for species coexistence, which corresponds to the red dot in Figure S8A. When σ is small ($\sigma \approx 0$), the probability of steady coexistence is 1, while this probability drops with increasing σ. When $\sigma = 0.45$, this probability approaches 0.1, and the supremum coexistence point of Δ, corresponds to a probability about 0.3. Obviously, $\Delta > 0$ (when D_i is the only different parameter between two consumer species) demonstrates a non-zero measure parameter space for coexistence and the value of $\Delta > 0$ manifests the likelihood for coexistence.

As shown in Figures S8A, B, D, R_0, the growth rate for biotic resource or R_a, the supply rate for abiotic resource, might play a critical role for the stability of the fixed point. To further demonstrate this point, we systematically studied the parameter space for stable coexistence. The results are shown in Figures 3 E-F and Figures S8E-H. Basically, scenarios involving different scenarios of chasing triplets (P-T Model and P-T Variants A-B) have qualitatively similar behavior. Here, the region below the blue surface and above the red surface are stable coexistence region, while the region below the red surface and above $\Delta = 0$ are the region for unstable fixed point. For abiotic resource cases, all fixed points are globally attracting and thus stable (Figure 3F and Figures S8G-H). For biotic resource cases, when the value of R_0 is small, there is a unstable fixed point region, where trajectories typically end in a limit cycle; when the value of R_0 is large, all fixed point are stable (Figure 3E and Figures S8E-F). Importantly, there is a non-zero parameter region for all models (P-T Model and P-T Variants A-B, biotic or abiotic resources) where the two consumer species can stably coexist (below the blue surface and above the red surface, Figures 3E-F and Figures S8E-H), which clearly demonstrates that the violation of CEP is not due to a special set of model parameters.

E Breaking CEP is parameter dependent

Forming chasing pairs and chasing triplets is not a guarantee for breaking CEP. From numerical solutions shown in Figure S10, the non-parallel surfaces may not own a common point in the feasible region (Figure S10A) (see Figure S10D for the time series), and the fixed point might be unstable (Figures S10B-C), which can end in an oscillating coexistence (see Figure S10B and the time series in Figure S10E) or one consumer species dies out (see Figure S10C and the time series in Figure S10F).

VI Breaking CEP for any number of resource species.

We have already illustrated that in case $N = 1$ and $M = 2$, both species of consumers can coexist at steady state and thus break the constraint of the CEP (Figures 2D, F and Figure S5D). Here we show that for any $N > 0$, the constraint of CEP can be liberated. When $N \geq 2$, we construct the following scenario that $M = N + 1$ species of consumers can coexist at steady state in a natural ecosystem: For consumer species C_i (i=1,...,$N-1$), each species only feeds on one resource species R_i (i=1,...,$N-1$), respectively. Meanwhile, consumer species C_N and C_{N+1} only feed on R_N. Then, similar to the case of $N = 1$ and $M = 2$, C_N and C_{N+1} can coexist. Meanwhile, similar to the case in Sec.I.A.2, species C_i (i=1,...,$N-1$) can coexist together with C_N and C_{N+1}. Consequently, all $N + 1$ species of consumers can coexist at steady state, with $M = N + 1 > N$.

VII Dimensional analysis for Models involving chasing triplets.

The equations for the population dynamics of P-T Model are shown in Equation 4 and Equation S18. For biotic resource cases:

$$\begin{cases} \dot{x_1} = a_1 R^{(\mathrm{F})} C_1^{(\mathrm{F})} - (d_1 + k_1)\, x_1 - b_1 x_1 C_1^{(\mathrm{F})} + e_1 y_1 \\ \dot{x_2} = a_2 R^{(\mathrm{F})} C_2^{(\mathrm{F})} - (d_2 + k_2)\, x_2 - b_2 x_2 C_2^{(\mathrm{F})} + e_2 y_2 \\ \dot{y_1} = b_1 x_1 C_1^{(\mathrm{F})} - (h_1 + e_1 + l_1)\, y_1 \\ \dot{y_2} = b_2 x_2 C_2^{(\mathrm{F})} - (h_2 + e_2 + l_2)\, y_2 \\ \dot{C}_1 = w_1 \left(k_1 x_1 + h_1 y_1\right) - D_1 C_1 \\ \dot{C}_2 = w_2 \left(k_2 x_2 + h_2 y_2\right) - D_2 C_2 \\ \dot{R} = R R_0 \left(1 - R/K_0\right) - \left(k_1 x_1 + h_1 y_1\right) - \left(k_2 x_2 + h_2 y_2\right) \end{cases} \tag{S38}$$

Define dimentionless variables $T, X_1, X_2, Y_1, Y_2, C_1', C_2', R', C_i^{(\mathrm{F})(\mathrm{dim})}, R^{(\mathrm{F})(\mathrm{dim})}$ as follows.

$$\begin{cases} T \equiv t/T_0; \\ X_1 \equiv x_1/x_{10}, X_2 \equiv x_2/x_{20}; \\ Y_1 \equiv y_1/y_{10}, Y_2 \equiv y_2/y_{20}; \\ C_1' \equiv C_1/C_{10}, C_2' \equiv C_1/C_{20}, R' \equiv R/r_0; \\ C_i^{(\mathrm{F})(\mathrm{dim})} \equiv C_i' - X_i - 2Y_i, \quad i = 1, 2; \\ R^{(\mathrm{F})(\mathrm{dim})} \equiv R' - \left(X_1 + X_2 + Y_1 + Y_2\right), \end{cases} \tag{S39}$$

and we define dimensionless parameters (marked with '$\equiv$') and chose the flexibe parameters as follow

$$\begin{cases} T_0 = N_1 (D_2)^{-1}, {R_0}' \equiv R_0 T_0, {D_1}' \equiv D_1 T_0, {D_2}' \equiv D_2 T_0 = N_1; \\ {e_i}' \equiv e_i T_0, {l_i}' \equiv l_i T_0, {k_i}' = k_i T_0, {h_i}' = h_i T_0, {d_i}' = d_i T_0, \quad i = 1, 2; \\ {a_1}' \equiv a_1 T_0 x_{10}, {a_2}' \equiv a_2 T_0 x_{10}, {b_1}' \equiv b_1 T_0 x_{10}, {a_2}' \equiv a_2 T_0 x_{10}; \\ r_0 = C_{10} = C_{20} = x_{10} = x_{20} = y_{10} = y_{20} = K_0/N_2. \end{cases} \tag{S40}$$

Here, N_1 and N_2 are two reducible parameters which can be either 1 or arbitrary positive numbers. Substituting Equations S39-.S40 into Equation S38, we get

$$\begin{cases} \dot{X}_i = {a_i}' {R^{(\mathrm{F})(\mathrm{dim})}} C_i^{(\mathrm{F})(\mathrm{dim})} - \left({d_i}' + {k_i}'\right) X_i - {b_i}' X_i C_i^{(\mathrm{F})(\mathrm{dim})} + {e_i}' Y_i \\ \dot{Y}_i = {b_i}' X_i C_i^{(\mathrm{F})(\mathrm{dim})} - \left({h_i}' + {e_i}' + {l_i}'\right) Y_i \\ \dot{{C_1}'} = w_1 \left({k_1}' X_1 + {h_1}' Y_1\right) - {D_1}' {C_1}' \\ \dot{{C_2}'} = w_2 \left({k_2}' X_2 + {h_2}' Y_2\right) - N_1 {C_2}' \\ \dot{R'} = R' \cdot {R_0}' (1 - R'/N_2) - \left({k_1}' X_1 + {h_1}' Y_1\right) - \left({k_2}' X_2 + {h_2}' Y_2\right) \end{cases} . \tag{S41}$$

Note that all variables and parameters in Equation S41 are dimensionless. Compare Equation S41 with Equation S38, it is clear that all equations have the same form except that N_1 and N_2 in Equation S41 are reducible which can be either 1 or arbitrary positive numbers. Similarly, for the abiotic resource case in P-T Model, or the biotic/abiotic resource cases in P-T Variants A-B, only two parameters: D_2 and K_0 are reducible in the dimensionless expressions, which can be set as either 1 or arbitrary positive numbers. For convenience, in our numerical calculations, we use the same parameter notation while they are all dimensionless parameters. For the choice of N_1 (D_2) and N_2 (K_0), in the biotic resource case, we set D_2=0.005, K_0=10; in the abiotic resource case, we set D_2=0.004, K_0=5.

Supplemental References

KELLEY, J. L. 2017. *General topology*, Courier Dover Publications.

NELSON, D. L. & COX, M. M. 2017. *Lehninger principles of biochemistry*, New York, W. H. Freeman.

ROHR, R. P., SAAVEDRA, S. & BASCOMPTE, J. 2014. On the structural stability of mutualistic systems.

Science, 345, 1253497.
ROY, S. & CHATTOPADHYAY, J. 2007. Towards a resolution of 'the paradox of the plankton': A brief overview of the proposed mechanisms. *Ecological Complexity*, 4, 26-33.
STRANG, G. 1993. *Introduction to linear algebra*, Wellesley-Cambridge Press Wellesley, MA.
THINGSTAD, T. & LIGNELL, R. 1997. Theoretical models for the control of bacterial growth rate, abundance, diversity and carbon demand. *Aquatic Microbial Ecology*, 13, 19-27.